The Canadian Mineralogist
Vol. 39, pp. 275-297 (2000)

ESTIMATES OF CRUSTAL ASSIMILATION IN QUATERNARY LAVAS FROM THE NORTHERN CORDILLERA, BRITISH COLUMBIA

JAMES K. RUSSELL§

Igneous Petrology Laboratory, Earth & Ocean Sciences, The University of British Columbia, Vancouver, British Columbia V6T 1Z4, Canada

STEINUNN HAUKSDÓTTIR

National Energy Authority, Grensasvegur 9, Reykjavik, IS-108, Iceland

Abstract

The region between the Iskut and Unuk rivers and immediately south of Hoodoo Mountain in northwestern British Columbia is host to eight distinct occurrences of Quaternary volcanic rocks comprising alkali olivine basalt and minor hawaiite. The centers range in age from 70, 000 to ~150 years B.P. This volcanic field, called herein the Iskut volcanic field, lies along the southern boundary of the Northern Cordilleran volcanic province (NCVP) and includes sites identified as: Iskut River, Tom MacKay Creek, Snippaker Creek, Cone Glacier, Cinder Mountain, King Creek, Second Canyon and Lava Fork. The lavas are olivine- and plagioclase-phyric, contain rare corroded grains of augite, and commonly entrain crustal xenoliths and xenocrysts. Many crustally derived xenoliths are partially fused. Petrological modeling shows that the major-element compositional variations of lavas within the individual centers cannot be accounted for by simple sorting of the olivine and plagioclase phenocrysts or even cryptic fractionation of higher-pressure pyroxene. Textural and mineralogical features combined with whole-rock chemical data suggest that assimilation of the underlying Cordilleran crust has affected the evolution of the relevant magmas. Mass-balance models are used to test the extent to which the within-center chemical variations are consistent with coupled crystallization and assimilation. On the basis of our analysis of four centers, the average ratio of assimilation to crystallization for the Iskut volcanic field is 1:2, suggesting that assimilation has played a greater role in the origins of NCVP lavas than recognized previously.

Keywords: magma, differentiation, crustal assimilation, geochemistry, modeling, Quaternary lavas, British Columbia.

Sommaire

La région entre les rivières Iskut et Unuk et immédiatement au sud du mont Hoodoo, dans le nord-ouest de la Colombie-Britannique, contient huit sites distincts d'effusion de lave quaternaire allant de basalte alcalin à olivine jusqu'à hawaiite (proportion mineure). Ces points d'effusion vont de 70, 000 à environ 150 ans avant aujoud'hui. Ce champ volcanique, que nous appelons Iskut, est situé le long de la bordure sud de la province volcanique de la Cordillère Nord, et inclut les sites de prélèvement déjà identifiés: Iskut River, Tom MacKay Creek, Snippaker Creek, Cone Glacier, Cinder Mountain, King Creek, Second Canyon et Lava Fork. Les laves ont cristallisé de l'olivine et du plagioclase comme phénocristaux, contiennent de rares grains corrodés d'augite, et entraînent assez couramment des xénolithes de croûte et des xénocristaux détachés. En plusieurs cas, ces xénolithes ont partiellement fondu. D'après nos modèles pétrologiques, les variations en composition globale des laves (éléments majeurs) aux différents sites ne pourraient être dues au simple triage des phénocristaux d'olivine et de plagioclase ou même au fractionnement cryptique d'un pyroxène de haute pression. Les aspects texturaux et minéralogiques des roches, considérés à la lumière des données chimiques sur roches globales, font penser que l'assimilation de la croûte sous-jacente de la Cordillère a affecté l'évolution du magma dans cette suite. Les modèles fondés sur le bilan des masses servent à tester la portée du couplage de la cristallisation et d'une assimilation pour expliquer les variations en compositions à quatre centres. D'après notre analyse, le rapport moyen de l'assimilation à la cristallisation serait 1:2, ce qui attribue un rôle plus important à l'assimilation que ce que l'on préconisait pour le cas des laves de la province volcanique de la Cordillère Nord.

(Traduit par la Rédaction)

Mots-clés: magma, différenciation, assimilation de la croûte, géochimie, modèle, laves quaternaires, Colombie-Britannique.

§ *E-mail address*: russell@perseus.geology.ubc.ca

Introduction

The Northern Cordilleran volcanic province (NCVP) comprises dominantly mafic, Neogene, alkaline volcanic rocks distributed across the northern Canadian Cordillera (Fig. 1). This magmatic province is situated west of the Tintina fault and east of the Denali–Coast fault system, and crosses four major tectonostratigraphic terranes: Stikinia, Cache Creek, Yukon–Tanana, and Cassiar (*cf.* Edwards & Russell 1999, 2000). NCVP magmatism is considered to be a product of extensional forces acting on the Northern Cordillera lithosphere. Recent work by Edwards & Russell (1999), for example, showed the timing and volumetric rates of NCVP magmatism to correlate with changes in the relative motions between the Pacific and North American plates, namely, a transition from dominantly compressional to dominantly transtensional.

NCVP magmas derive from asthenospheric mantle sources situated beneath the Canadian Cordillera (Francis & Ludden 1990, Carignan *et al.* 1994, Cousens & Bevier 1995, Moore *et al.* 1995, Edwards & Russell 2000). The mineralogy and chemical compositions of these lavas, therefore, have the capacity to serve as im-

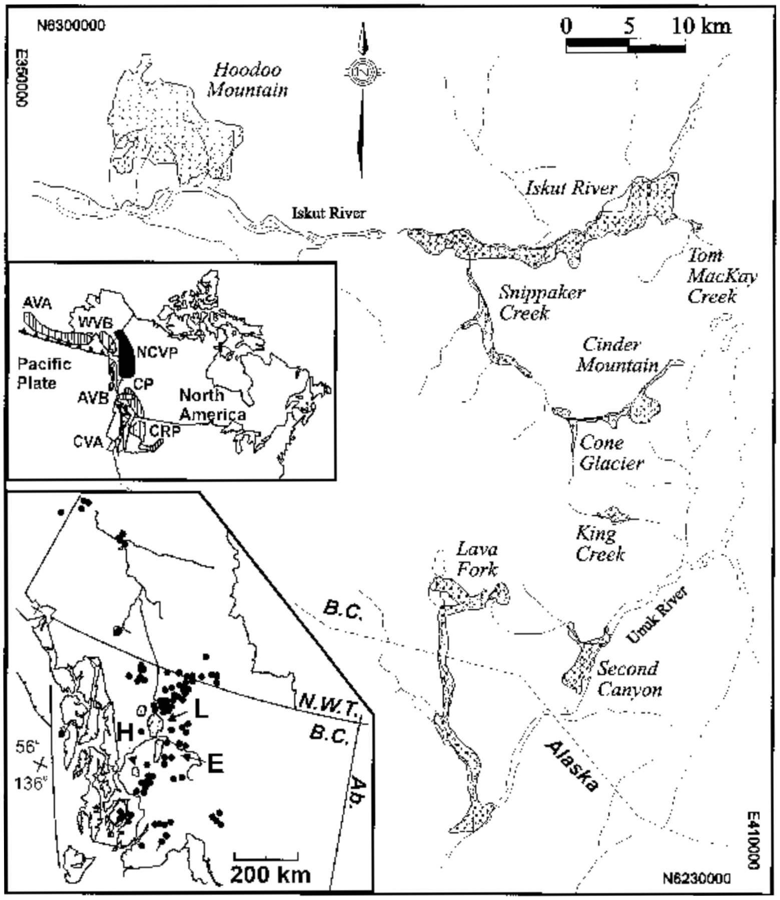

FIG. 1. Map showing the distribution of Quaternary volcanic rocks in the region of the Iskut and Unuk rivers, including the Hoodoo Mountain volcanic complex, northwestern British Columbia. Coordinates are for UTM Zone 9. Lower inset shows distribution of Neogene to Quaternary volcanic rocks within the Northern Cordilleran volcanic province (NCVP; Edwards & Russell 1999, 2000, Souther 1990a) including Level Mountain (L), Edziza (E) and Hoodoo Mountain (H). Upper inset shows the distribution of other major volcanic provinces along the western margin of North America: Aleutian arc (AVA), Wrangell volcanic belt (WVB), Anaheim volcanic belt (AVB), Chilcotin plateau (CP), Cascade arc (CVA) and Columbia River plateau (CRP).

portant indicators of variations in the underlying mantle. However, it is equally clear that the primary asthenosphere-derived magmas must traverse a complicated, diverse and poorly known column of lithosphere. Lithosphere to the Northern Cordillera potentially comprises both autochthonous and allochthonous blocks of crust and mantle. Consequently, if the NCVP volcanic rocks are to be used as probes to the underlying asthenosphere, it is essential that we recognize and quantify the effects of crustal assimilation.

In this paper, we explore this problem through study of Quaternary lavas from volcanic centers situated between the Iskut and Unuk rivers (Fig. 1) near the southern margin of the NCVP. The lavas include alkali olivine basalt and minor hawaiite, and they commonly contain xenoliths and xenocrysts of crustal derivation. The chemical diversity within and between individual centers is shown to be inconsistent with closed-system processes alone (*e.g.*, fractionation) and requires assimilation of crustal material. Our analysis places confidence limits on the amounts of crystallization and assimilation represented by the compositional range of lavas at individual centers. We suggest that the mass ratios of material fractionated (*e.g.*, phenocrysts) to that assimilated for this part of the NCVP is constant. This relationship between the extents of crystallization and assimilation may reflect the crustal architecture of this region of the Cordillera.

Background Information

The Iskut volcanic field comprises eight individual Quaternary volcanic centers situated between the Iskut and Unuk rivers of northwestern British Columbia (Table 1, Fig. 1). It is located within the Boundary Ranges of the Coast Mountains, near the boundary between the Coast and Intermontane physiographic belts. The field is situated in the southern part of the NCVP (Fig. 1) and is immediately southeast and southwest of two large composite volcanoes: Hoodoo Mountain (Edwards & Russell 1994, Edwards 1997) and Edziza (Souther 1992), respectively. The centers comprising the Iskut volcanic field (Fig. 1) include (from north to south): Iskut River (IR), Tom MacKay Creek (TMC), Snippaker Creek (SNC), Cone Glacier (CG), Cinder Mountain (CM), King Creek (KC), Second Canyon (SC) and Lava Fork (LF). Volcanism across the Iskut volcanic field spans (at a minimum) 70,000 to 150 years B.P., making these lavas some of the youngest in Canada (Table 1).

The region is underlain, in part, by the Stikinia terrane, an allochthonous suite of late Paleozoic and Mesozoic volcanic, plutonic and sedimentary rocks considered to have formed in an island-arc setting (Monger 1984, Gabrielse & Yorath 1991). Specifically, the Quaternary volcanic rocks overlie basement comprising the Paleozoic Stikine assemblage, Upper Triassic Stuhini Group, Lower to Middle Jurassic volcanic and sedimentary rocks of the Hazelton Group, and Middle to Upper Jurassic sedimentary rocks of the Bowser Lake Group, all of which are intruded by Devonian, Triassic, Jurassic and Tertiary plutons (Britton *et al.* 1989, Wheeler *et al.* 1988, Wheeler 1991, Anderson 1993).

Volcanic centers belonging to the Iskut field were first described by regional mapping programs (*e.g.*, Wright 1906, Kerr 1948). Grove (1974, 1986) provided the first comprehensive study of these Quaternary volcanic rocks, including petrographic descriptions and chemical analyses. At present, the most detailed mapping of these volcanic centers derives from unpublished BC Hydro reports compiled between 1982 and 1984, as part of the Iskut Canyon and More Creek hydroelectric projects. That work addressed the Recent geological history of the area and provided 1:50,000 and 1:10,000 scale geological mapping supported by ^{14}C and K–Ar dating and diamond drilling of lava flows from the Iskut River center. Regional geological mapping programs (Britton *et al.* 1988, 1989, Read *et al.* 1989) further re-

TABLE 1. GENERAL VOLCANOLOGICAL INFORMATION ON CENTERS FROM THE ISKUT VOLCANIC FIELD

Centre	Label	Age (years)	Method	Rock Type	Vents	Surface area (km^2)	Volume Estimates (km^3)
Iskut River	IR	70 000 ± 30 000 to 2 555 ± 60	K-Ar & ^{14}C	Basalt	3	37.5	0.75 - 4.8
Tom MacKay Creek	TMC	Recent	-	Basalt	1	0.4	< 0.012
Snippaker Creek	SNC	Recent	-	Basalt	1	6.2	0.06 - 0.12
Cone Glacier	CG	Recent	-	Basalt	2	4.3	0.02 - 0.065
Cinder Mountain	CM	33 000 ± 2 400[1]	^{14}C	Basalt Hawaiite	1	5.4	0.03 - 0.05
King Creek	KC	Recent	-	Basalt	1	1.3	< 0.07
Second Canyon	SC	Recent	-	Basalt	2	8.6	0.03 - 0.13
Lava Fork	LF	360 ± 60 to ~150	^{14}C, tree rings	Basalt	2	21.9	0.02 - 0.22

[1] Date from Copper King Creek lava flow.

fined the distributions of Recent volcanic rocks in the Snippaker Creek and Unuk River areas. Elliott *et al.* (1981) described lava flows and stratigraphic relationships at the Lava Fork center (*e.g.*, Souther 1990b). Stasiuk & Russell (1990) and Hauksdóttir *et al.* (1994) revised field relationships and geological maps and identified two additional volcanic centers. Bevier (1992) and Cousens & Bevier (1995) presented trace-element data and Sr, Nd and Pb isotopic data for four of the volcanic centers. On the basis of these data, they suggested an origin involving contamination of primary magmas by lithospheric mantle or by arc-related crustal rocks of Stikinia.

The challenge of distinguishing chemical traits due to asthenospheric source-regions from those traits incurred by interaction with lithosphere is a real one (Carter *et al.* 1978, DePaolo 1981, Brandon *et al.* 1993). However, in the Northern Cordillera, the task is further complicated because the underlying crust, and perhaps parts of the lithospheric mantle, comprise Late Paleozoic to Mesozoic, arc-derived material that features relatively juvenile trace element and isotopic compositions (*e.g.*, Eiché *et al.* 1987, Bevier 1992, Glazner & Farmer 1992, Carignan *et al.* 1994, Cousens & Bevier 1995, Edwards & Russell 2000). Many of the volcanic rocks that make up Stikinia, for example, have $^{87}Sr/^{86}Sr$ less than 0.707 and are isotopically indistinguishable from NCVP volcanic rocks and some modern-day ocean-island basalt (*e.g.*, Samson *et al.* 1989, Cousens & Bevier 1995, Carignan *et al.* 1994, Edwards & Russell 2000).

Volcanic Centers

The Iskut River center comprises plagioclase + olivine porphyritic basalt lava flows and minor cinder (Fig. 1). Recent flows have filled an ancient canyon formed by the paleo-Iskut River. The present-day Iskut River is recovering the original drainage by cutting down through the thick (>100 m) sequence of flows and creating the Iskut Canyon. Flows at the base of the Iskut River volcanic center are approximately 70,000 years old, on the basis of K–Ar dating; the overlying basalt flows are dated at 8730 years (^{14}C) (Table 1; Read *et al.* 1989). Relatively younger ash deposits are dated at 2555 ± 60 years (^{14}C); the stratigraphically youngest units have not been dated, however.

A single flow unit composed of highly jointed and fragmented pillow basalt occurs in Tom MacKay Creek, east of the Iskut River lavas (Fig. 1). The lavas are plagioclase- and olivine-phyric and contain phenocrysts up to 3–6 mm in size. Individual pillows are 20–40 cm in diameter, highly vesicular, radially jointed and commonly have a glassy rind. Locally, these accumulations of pillow basalt form cliffs 20–30 m high; these are interpreted as products of subaqueous eruption against or close to ice.

Recent flows of basalt lava outcrop within the Snippaker Creek drainage (Fig. 1, Table 1). Lava flows were sampled in narrow, steep-sided canyons at the southern terminus, the mid-point along Memorial Creek close to the probable vent, and at the northern terminus. The sections comprise up to six flows, each at least 3–5 m thick. The flow units are indistinguishable; they have grey, vesicular, fresh surfaces and are porphyritic, with 0.1 to 1 cm phenocrysts of plagioclase and olivine.

The Cone Glacier volcanic center (CG; Fig. 1, Table 1) comprises interbedded basaltic lava flows, pillow lava and scoriaceous cinder breccias centered around two prominent cinder cones. Cone Glacier lavas cover a portion of Snippaker Creek (to the west) and underlie the King Creek – Julian Lake drainage (to the south). The Cone Glacier lavas are characterized by abundant megacrysts (1–3 cm) of euhedral, vitreous-looking plagioclase, but they also contain smaller phenocrysts of olivine and plagioclase. The plagioclase megacrysts serve to distinguish volcanic rocks of Cone Glacier from Cinder Mountain lavas.

Cinder Mountain is located immediately east and northeast of Cone Glacier (Fig. 1) and comprises hyaloclastite breccia, pillowed lava and dykes. The massive rocks are light grey in color, intermediate in composition, and aphanitic except for rare feldspar microphenocrysts. The eastern edge of the Cinder Mountain field is marked by an isolated remnant of a basaltic lava flow 15–20 m thick, outcropping close to Copper King Glacier near the head of Harrymel Creek. This lava contains olivine and plagioclase phenocrysts but lacks the megacrysts of plagioclase that characterize the Cone Glacier lavas.

The King Creek center is dominated by olivine- and plagioclase-phyric basaltic pillow lavas and associated breccias (Fig. 1, Table 1). The lavas are exposed in a steep narrow creek bed, where they form a cliff 40–50 m high. A 1–2-m-wide vertical dyke cross-cuts the pillow lavas. The restricted extent of this relatively thick package of pillow lava and the associated breccia suggests a subaqueous environment related to eruption beneath or against ice (*cf.* Tom MacKay Creek).

The Second Canyon occurrence comprises a blocky-surfaced, columnar-jointed basalt lava flow and a cone located on Canyon Creek (Fig. 1; Stasiuk & Russell 1990). The lava is olivine-phyric and contains <5% plagioclase microphenocrysts.

The Lava Fork volcanic field is situated at the confluence of Blue and Unuk rivers (Fig. 1, Table 1) and comprises a series of basalt lava flows and associated tephra. The lavas are olivine- and plagioclase-phyric and are probably the youngest volcanic rocks in the Canadian Cordillera. The youngest flows erupted from a vent located on a ridge on the northeastern side of Lava Fork valley. The older flows derive from a vent marked by a cone located 4 km downstream of Blue Lake. A minimum age of 360 ± 60 years B.P. is attributed to one of the flows on the basis of ^{14}C dating of a conifer log on the surface of one of the flows (Elliott *et al.* 1981). Tree-ring counts on living trees yield minimum ages of 150 years for the youngest flow and 350 years for the older flows.

Petrography

Alkali olivine basalts

The Iskut lavas consist of basalt, except for the Cinder Mountain lavas, which are hawaiite. The basaltic rocks are petrographically similar; they are 10–35% vesicular and contain 5–30% phenocrysts of plagioclase and olivine. All basalts have a groundmass of plagioclase, olivine, augite (usually titanaugite), Fe–Ti oxides and apatite. Both magnetite and ilmenite occur in the groundmass of all volcanic rocks.

Olivine phenocrysts and microphenocrysts are generally euhedral to subhedral, up to 3 mm in size and comprise 3–15% of the rock. Olivine contains spinel inclusions. Partially resorbed grains of olivine (phenocrysts or xenocrysts) are rare but occur in samples from IR, SNC, CG, and CM centers. The corroded olivine is probably cognate on the basis that it does not have a composition typical of mantle-derived olivine.

Plagioclase is the most voluminous phase and invariably occurs as a phenocryst and as a groundmass phase. Many basalts carry 0.5 to 2 cm vitreous-looking plagioclase crystals that show prominent twinning. In fact, one of the more distinctive features of the Iskut lavas is the diversity of habits and textures of plagioclase commonly found within a single flow. Megacrysts exceed 1 cm in size, are euhedral, and commonly show prominent twinning and multiple internal-dissolution surfaces. They generally have a homogeneous core enveloped by narrow, strongly zoned rims. Phenocrysts and microphenocrysts are texturally diverse, and most contain complex internal-dissolution surfaces and are strongly zoned. A separate group of strongly zoned phenocrysts is distinguished by the presence of sieved interiors. Groundmass plagioclase is twinned, normally zoned and lacks internal-dissolution surfaces. Megacrysts and sieved phenocrysts are found in most centers, but both are absent in lavas from CM, SC, LF centers.

Clinopyroxene occurs in the groundmass of all lavas as small tabular, colorless to brown–purple pleochroic laths and as subophitic masses. Rare grains of partly resorbed clinopyroxene, up to 0.3 mm in size, occur in basalt from at least four volcanic centers (IR, TMC, CG, KC). Rare clinopyroxene is also found as inclusions in plagioclase megacrysts. The last occurrence suggests a cognate rather than a xenocrystic origin.

Hawaiite

The majority of Cinder Mountain lavas are hawaiite in composition. They contain anhedral (1–4 mm) phenocrysts of andesine and minor olivine in a subtrachytic groundmass of plagioclase, magnetite and some apatite. Olivine microphenocrysts (<1 mm) are euhedral to subhedral and commonly contain melt and oxide inclusions. One sample of hawaiite contains 1–2 mm grains of olivine that are strongly embayed and corroded. Apatite also occurs as 0.2 mm microphenocrysts and is usually associated with magnetite.

Plagioclase phenocrysts commonly show resorption textures. Twinned plagioclase phenocrysts show multiple, distorted, narrow and discontinuous twin-planes. The complex twinning and anhedral form of the plagioclase phenocrysts are distinctive relative to plagioclase from other centers. At least some of the larger plagioclase crystals seem to be corroded xenocrysts from crustal rocks and exhibit an inherited twinning that is partially annealed.

Xenoliths

Xenoliths and xenocrysts derived from felsic plutonic rocks and schists are common in lavas from the Iskut volcanic field. Granitic xenoliths and xenocrysts of quartz and feldspar are common in lavas from Iskut River, Snippaker Creek, Cone Glacier, King Creek, and in the basalt flow near Coppermine Glacier (*e.g.,* Cinder Mountain). Lava Fork basalts contain abundant plutonic (granite) and metamorphic (*e.g.*, mafic schist, felsic gneiss) xenoliths ranging in size from 5 to 30 cm. In some instances, the xenoliths correspond to basement rock-types found within the region. For example, biotite granite and schist underlie much of the area immediately around the Lava Fork center, and these rock types are found as xenoliths in the lavas (see below).

In general, xenoliths are angular to rounded, and many are partly fused, or have reacted with the host magma, or have been invaded by magma (*e.g.,* Al-Rawi & Carmichael 1967, Sigurdsson 1968). Fused xenoliths are glassy, variably vesiculated and may even show radially oriented jointing (*e.g.,* perpendicular to the edges of the xenolith). Granitic xenoliths in Lava Fork basalts (*e.g.,* SH–41) commonly occur as white blocks of highly vesicular to frothy glass. In thin section, the glass is nearly colorless and can constitute 60–90% by volume of the sample. Relict primary minerals are represented by rounded grains of quartz and microcline. In other less thoroughly melted samples, glass is commonly concentrated at grain boundaries. The boundary between granitic and basaltic material is generally sharp, but locally, basaltic melt has mixed with the felsic melt to produce a streaky, colored glass (*cf.* Maury & Bizouard 1974).

Xenoliths of mafic schist from Lava Fork show preferential melting along relict foliation planes (*e.g.,* SH–42). In these xenoliths, glass is vesicular and occurs in thin (<3 mm) layers separated by more strongly quartzofeldspathic layers. The glass is brown and heterogeneous in color, and seems to be produced mainly by melting of a biotite-rich assemblage found along foliation planes. Analysis by scanning electron microscope shows some relict pseudomorphs of biotite to be composed of iron oxides (*i.e.,* Kaczor *et al.* 1988, Le Maitre

1974). Within the quartzofeldspathic layers, feldspar commonly shows partial melting along the cleavages.

Mineral and Glass Chemistry

Analytical methods

Mineral and glass compositions were measured on polished thin sections using a Cameca SX–50 electron microprobe at the University of British Columbia. All compositions were determined under operating conditions of 15 kV and 20 nA, with peak counting times of 20 seconds. Off-peak background counts were collected for 10 seconds. A standard beam 2–5 μm in diameter was used for the analysis of olivine, pyroxene and plagioclase. Standards included: albite (Na,Al), orthoclase (K), forsterite (Mg), fayalite (Fe), diopside (Ca,Si), chromite (Cr), rutile (Ti), Ni_2SiO_4 (Ni) and rhodonite (Mn). Glass compositions were measured using a reduced current (5 nA) and a defocussed beam (15 μm).

Olivine

Basalt lavas contain olivine phenocrysts ranging in composition from Fo_{84} to Fo_{61}. Groundmass olivine shows a similar range in composition ($Fo_{81–55}$). The most magnesian olivine (Fo_{84}) is found in lavas from Second Canyon, Tom MacKay Creek, and King Creek. Olivine within the Iskut lavas invariably contains greater than 0.1 wt% CaO.

Olivine from Cinder Mountain hawaiite is substantially more Fe-rich. Olivine phenocrysts vary from Fo_{54} to Fo_{33}. One sample of hawaiite (CM–21) contains rare sieve-textured olivine that shows reverse core-to-rim compositional zoning (Fo_{33} to Fo_{52} rim). The core composition of this olivine is the most iron-rich observed in the entire suite of samples.

Plagioclase

Compositions of plagioclase megacrysts and phenocrysts in the basalt lavas span the limits of labradorite and andesine (An_{74} to An_{45}). Samples from the Iskut River center contain rare xenocrysts of anorthite (An_{94}). Sieve-textured plagioclase phenocrysts commonly show reverse zoning, having core compositions of $An_{44–48}$ and rim compositions of $An_{50–70}$. The groundmass plagioclase (An_{38} to An_{68}) overlaps the compositional range found in plagioclase (micro-)phenocrysts. Hawaiite samples from Cinder Mountain contain microphenocrysts that range from An_{39} to An_{50}; the groundmass plagioclase has higher average An-content ($An_{45–48}$).

Clinopyroxene

Pyroxene is mainly a groundmass constituent in lavas from the Iskut volcanic field, except for the rare occurrences as partly corroded, brown-colored grains (*e.g.*, xenocrysts) or as inclusions within phenocrysts of plagioclase. All pyroxene lies within the augite–titanaugite composition field. Groundmass clinopyroxene from King Creek lavas contains as much as 6 wt.% TiO_2. The Mg number (Mg#) for groundmass augite is between 75 and 46, whereas xenocrystic augite has a more restricted Mg#, 76–75. Augite xenocrysts also have higher ^{IV}Al and substantially lower Ti^{4+} contents relative to groundmass augite. The higher ^{IV}Al contents are consistent with crystallization at higher pressures (*e.g.*, Kushiro 1960, Le Bas 1962).

Whole-Rock Geochemistry

All samples were analyzed for major, minor, trace, and rare-earth elements (Tables 2, 3, 4). Preparation of sample powders followed procedures described by Cui & Russell (1995). Major-element and trace-element abundances (Table 2) were determined at the Geochemical Laboratories of McGill University by X-ray fluorescence (XRF) spectrometry using a Philips PW2400 spectrometer. Major-element concentrations were established with fused sample powders fluxed with lithium metaborate; concentrations of trace elements were measured on pressed powder pellets. Ferrous iron and $H_2O(T)$ contents were measured in the Igneous Petrology Lab at The University of British Columbia by volumetric analysis and by the Penfield method, respectively. The analytical uncertainty on major-element concentrations was established by replicate (N = 5) analysis of the powder for sample CG–9 (Table 2). All measurements of CO_2 and a subset of FeO and $H_2O(T)$ determinations were made at the Geological Survey of Canada (Ottawa); CO_2 and $H_2O(T)$ were measured by combustion followed by infrared spectrometry. Rare-earth element (*REE*) concentrations for a subset of samples (Table 4) were measured on an Elan-5000 inductively coupled plasma – mass spectrometer (ICP–MS) at the Department of Geological Sciences at the University of Saskatchewan (Jenner *et al.* 1990). Sample SH–39 was analyzed in duplicate to provide a measure of analytical variance on *REE* abundances (Table 4). Rare-earth-element contents for the entire suite were also measured by ICP–MS at the Geological Survey of Canada in Ottawa.

Major-element composition

Lavas from the Iskut volcanic field have alkaline compositions (Fig. 2) and are slightly nepheline- or hypersthene-normative. The suite contains 46 to 50 wt.% SiO_2, between 9.6 and 2.9 wt.% MgO, 12.5 to 14.7 wt.% $Fe_2O_3(T)$, and 2 to 3.2 wt.% TiO_2 (Fig. 3). The calculated solidification index (S.I., Table 3) ranges from 35 for the most primitive sample (Second Canyon) to 11 for hawaiite from Cinder Mountain (Fig. 3). The uncorrected Mg# (Table 2) for basalt samples ranges from 67.4 to 53.5, except for a single sample that shows

TABLE 2. MAJOR AND TRACE ELEMENT CONTENTS OF LAVAS FROM THE ISKUT VOLCANIC FIELD

Centre	Iskut River								TMC	Snippaker Creek				
Sample	IR-2	IR-3	IR-4	IR-5	IR-6	IR-7	IR-8	SH-37	SH-39	SH-01	SH-02	SH-31	SH-33	SH-34
SiO_2	48.95	48.84	47.99	48.02	49.09	48.80	47.98	48.90	48.01	48.63	48.48	48.37	48.50	47.67
TiO_2	2.33	2.24	2.32	2.25	2.35	2.36	2.20	2.38	2.30	2.33	2.30	2.28	2.31	2.27
Al_2O_3	16.32	16.78	16.87	16.93	16.29	16.38	17.04	16.35	15.55	16.74	16.84	16.81	16.78	16.06
Fe_2O_3	3.67	3.95	2.36	2.39	2.66	3.10	2.16	3.47	3.26	2.68	2.31	2.93	2.99	5.69
FeO	8.11	7.74	9.47	9.31	9.01	8.71	9.37	8.40	8.50	9.00	9.40	8.70	8.80	6.70
MnO	0.19	0.18	0.18	0.19	0.19	0.19	0.17	0.18	0.18	0.18	0.18	0.18	0.18	0.19
MgO	6.14	6.38	6.74	6.94	6.14	6.36	7.01	6.15	7.82	6.13	6.26	6.40	6.29	7.32
CaO	8.93	8.79	9.19	9.39	8.95	9.09	9.32	8.97	10.01	9.27	9.33	9.45	9.19	9.58
Na_2O	3.45	3.42	3.82	3.70	3.89	3.64	3.63	3.55	2.90	3.51	3.36	3.55	3.54	3.43
K_2O	1.16	1.08	0.91	0.87	1.19	1.10	0.86	1.15	0.94	1.00	0.95	0.91	0.98	0.84
P_2O_5	0.45	0.49	0.41	0.38	0.46	0.45	0.36	0.47	0.38	0.41	0.40	0.38	0.41	0.37
Total	99.71	99.89	100.27	100.36	100.22	100.18	100.11	99.97	99.85	99.88	99.81	99.96	99.97	100.12
H_2O_T	0.26	0.31	0.38	0.33	0.34	0.25	0.25	0.30	0.70	0.30	0.20	0.10	0.10	0.20
CO_2	0.30	0.20	0.10	0.20	0.20	0.20	0.20	0.20	0.20	0.20	0.10	0.20	0.20	0.10
MG#[3]	57.43	59.52	55.92	57.06	54.85	56.55	57.14	56.62	62.12	54.84	54.28	56.73	56.03	66.07
S.I.[4]	27.24	28.27	28.92	29.91	26.83	27.76	30.43	27.07	33.38	27.47	28.09	28.45	27.83	30.52
Trace elements														
Ba (ppm)	501	474	327	298	455	438	291	475	253	347	372	277	378	285
Ce	92	53	49	38	73	95	74	41	47	62	77	86	57	60
Co	42	50	53	52	42	41	42	45	48	42	45	45	48	58
Cr	26	14	17	16	26	27	6	32	60	21	21	30	24	31
Cu	8	53	98	44	77	51	87	48	49	66	46	76	51	77
Nb[1]	24	24	23	18	24	21	20	23	23	22	18	21	21	25
Ni	57	54	56	110	47	50	48	46	65	39	42	51	42	49
Rb[1]	17	22	20	20	25	17	16	17	14	13	12	16	13	23
Sc	26	31	17	39	34	37	28	33	38	29	27	37	29	34
Sr[1]	610	660	650	650	610	620	650	610	580	630	630	640	620	600
V	234	216	227	227	226	239	213	230	253	228	227	217	225	244
Zn	113	110	106	102	110	108	105	109	96	108	105	106	107	104
Zr[1]	210	200	180	170	210	210	170	220	170	200	200	180	190	230
Norms														
Or	6.86	6.38	5.38	5.14	7.03	6.50	5.08	6.80	5.56	5.91	5.61	5.38	5.79	4.96
Ab	29.19	28.94	27.53	27.17	30.55	30.80	27.18	30.04	24.54	29.70	28.43	29.74	29.95	29.02
An	25.62	27.25	26.20	27.02	23.48	25.11	27.67	25.29	26.64	26.97	28.07	27.25	27.01	25.95
Ne	-	-	2.59	2.24	1.28	-	1.91	-	-	-	-	0.16	-	-
Di	12.78	10.64	13.68	13.96	14.66	13.89	13.26	13.13	16.62	13.37	12.80	13.98	12.97	15.16
Hy	6.52	8.31	-	-	-	0.19	-	3.91	5.06	1.52	2.77	-	1.44	3.25
Ol	7.96	7.26	16.11	16.24	13.85	13.68	16.86	10.18	11.48	13.16	13.50	13.93	12.98	7.73
Mt	5.32	5.73	3.43	3.46	3.85	4.49	3.14	5.02	4.73	3.88	3.35	4.50	4.87	10.33
Hm	-	-	-	-	-	-	-	-	-	-	-	-	-	-
Il	4.42	4.25	4.41	4.27	4.46	4.48	4.18	4.52	4.37	4.42	4.37	4.33	4.39	4.31
Ap	1.07	1.16	0.97	0.90	1.09	1.07	0.85	1.11	0.90	0.97	0.95	0.90	0.97	0.88

[1] Analyzed by Geological Survey of Canada (GSC), Ottawa.

[2] Ferrous iron and water determined by GSC for all SH-xx samples; FeO for other samples analyzed at UBC.

[3] Mg# = 100*MgO/(MgO+FeO) in moles.

[4] S.I. = 100*MgO/(MgO+FeO+Fe_2O_3+Na_2O)+K_2O)

TABLE. 2 CONT'D

Cone Glacier														
CG-9	CG-10	CG-11	CG-12	CG-13	CG-14	CG-15	CG-18	SH-13	SH-14	SH-15	SH-22	SH-26	CM-19	CM-20
48.55	48.36	49.00	49.05	47.85	48.54	48.34	47.64	49.35	47.95	47.82	47.06	47.26	49.64	49.30
2.23	2.25	2.26	2.37	2.39	2.33	2.33	2.43	2.37	2.16	2.28	2.73	2.72	2.28	2.25
17.06	16.88	16.93	16.56	15.82	16.91	16.72	15.83	16.38	16.21	16.12	16.21	16.33	16.05	15.92
3.62	2.16	3.88	4.34	2.46	4.32	4.31	2.40	4.25	8.20	6.02	5.34	6.95	4.85	4.95
7.87	9.43	7.70	7.58	9.26	7.47	7.57	9.49	7.70	4.10	6.30	8.20	6.70	8.34	8.15
0.18	0.18	0.18	0.19	0.19	0.19	0.18	0.19	0.19	0.18	0.18	0.20	0.20	0.25	0.25
6.34	6.55	5.87	5.62	7.38	5.96	5.98	7.39	5.77	7.61	7.31	6.30	6.32	3.07	3.05
9.48	9.41	9.14	8.64	9.32	9.27	9.23	9.35	8.60	9.61	9.63	8.78	8.84	6.46	6.27
3.71	3.47	3.67	3.75	3.28	3.50	3.61	3.27	3.73	3.25	3.27	3.51	3.54	4.56	4.46
0.92	0.92	1.05	1.19	1.09	0.97	0.97	1.18	1.24	0.80	0.83	0.93	0.94	2.58	2.59
0.38	0.39	0.41	0.46	0.46	0.41	0.41	0.47	0.47	0.34	0.36	0.42	0.43	1.53	1.49
100.34	100.00	100.08	99.75	99.51	99.88	99.65	99.63	100.05	100.41	100.12	99.68	100.23	99.61	98.67
0.25	0.24	0.17	0.22	0.34	0.40	0.25	0.56	0.10	0.20	0.30	0.10	0.20	0.45	2.01
0.10	0.10	0.10	0.10	0.10	0.30	0.20	0.10	0.20	0.10	0.10	0.10	0.20	0.10	0.60
58.94	55.32	57.62	56.94	58.68	58.71	58.48	58.13	57.19	76.79	67.41	57.80	62.71	39.62	40.03
28.22	29.07	26.49	25.00	31.43	26.81	26.65	31.15	25.43	31.76	30.81	25.95	25.84	13.12	13.15
Trace elements														
281	302	338	454	339	376	355	340	489	226	248	270	347	905	881
90	61	55	78	78	72	42	60	58	68	61	43	111	149	145
44	40	35	39	42	37	39	48	32	46	46	50	55	25	26
25	31	20	18	36	27	26	29	18	28	29	10	13	0	0
50	62	47	47	45	57	29	46	41	67	39	70	42	59	42
20	21	22	25	28	22	19	25	25	20	19	23	22	54	55
49	69	33	35	65	40	41	63	41	65	59	39	38	20	18
18	17	16	28	17	16	20	17	23	17	13	11	12	36	41
31	27	36	36	44	34	30	32	28	43	35	32	33	31	27
640	630	630	630	590	630	630	600	600	600	590	620	630	650	620
226	221	214	221	235	227	238	228	226	222	229	247	255	82	61
105	106	107	115	104	110	110	108	115	101	105	123	118	164	164
180	180	200	230	210	200	200	210	230	180	180	200	200	420	420
Normative mineralogy														
5.44	5.44	6.21	7.03	6.44	5.73	5.73	6.97	7.33	4.73	4.91	5.50	5.56	15.25	15.31
30.30	28.71	31.05	31.73	27.25	29.61	30.54	25.85	31.56	27.50	27.67	29.70	29.95	38.58	37.74
27.19	27.77	26.63	24.84	25.23	27.57	26.56	25.04	24.29	27.28	26.86	25.73	25.90	15.71	15.78
0.59	0.35	-	-	0.27	-	-	0.98	-			-	-	-	-
14.07	13.41	13.00	12.15	14.67	12.71	13.37	14.91	12.38	14.15	14.70	12.15	11.98	5.26	4.63
-	-	3.06	4.90	-	5.41	2.81	-	5.60	8.82	6.35	3.23	5.89	1.09	3.06
12.40	16.02	9.28	7.24	16.48	7.21	9.01	16.72	7.14	2.50	5.76	9.48	4.73	8.83	7.27
5.25	3.13	5.62	6.29	3.57	6.27	6.25	3.47	6.16	7.58	8.72	7.74	10.08	7.03	7.17
-	-	-	-	-	-	-	-	-	2.97	-	-	-	-	-
4.23	4.27	4.29	4.50	4.54	4.42	4.42	4.61	4.50	4.10	4.33	5.18	5.17	4.33	4.27
0.90	0.92	0.97	1.09	1.09	0.97	0.97	1.11	1.11	0.81	0.85	0.99	1.02	3.62	3.53

an anomalously high degree of oxidation. Hawaiite from Cinder Mountain has an Mg# between 48 and 34.

Geochemistry of fused xenoliths

The chemical compositions for representative xenoliths from Lava Fork, the compositions of glass derived from the partial fusion of the same xenoliths, and the composition of a locally outcropping quartz monzonite (LF–28) are reported in Table 3. The xenolith of granite (SH–41) and xenolith LF–28 have similar compositions, but the metamorphic xenolith (SH–42) is substantially poorer in alkalis (Table 3). In the majority of cases, glass within the fused granitic xenolith is colorless, and its composition plots within the field of end-member feldspar compositions (An–Ab–Or), near the Ab–Or join (Fig. 4). This trend results from melts being produced mainly by fusion of alkali feldspar and minor amounts of Fe–Mg hydrous phases. A subset of the glass is light brown and plots toward the field of basalts (Fig. 4).

TABLE 2. CONT'D

Cinder Mountain				KC	SC	Lava Fork							1 σ
CM-21	SH-19	SH-21	SH-35	KC-22	SC-23	LF-24	LF-30	LF-31	LF-32	SH-44	SH-54	SH-60[1]	(N=5)
50.07	49.70	50.18	47.37	49.35	46.06	46.44	46.41	46.48	46.77	46.46	46.44	46.47	0.195
2.21	2.26	2.16	3.24	2.24	2.57	2.84	2.83	2.81	2.77	2.84	2.83	2.84	0.013
16.09	16.04	16.04	16.04	16.55	14.89	16.94	16.86	16.92	16.90	16.92	16.97	16.94	0.114
3.85	3.18	3.25	3.46	2.77	4.30	4.92	3.62	2.72	2.67	2.59	4.90	3.28	0.045
9.12	9.80	9.80	10.00	8.50	8.28	7.91	9.16	9.91	9.86	10.10	7.90	9.40	0.020
0.25	0.25	0.26	0.21	0.18	0.18	0.18	0.18	0.18	0.18	0.18	0.18	0.18	0.005
2.94	2.99	2.81	5.21	6.00	9.25	6.50	6.52	6.62	6.71	6.52	6.56	6.55	0.040
6.29	6.32	6.17	8.31	8.56	10.24	8.95	8.89	8.87	8.81	8.87	8.91	8.88	0.023
4.54	4.88	4.81	3.93	3.75	2.85	3.59	3.56	3.64	3.86	3.71	4.00	3.68	0.010
2.71	2.63	2.76	1.21	1.38	0.91	1.09	1.09	1.08	1.09	1.09	1.08	1.10	0.007
1.47	1.52	1.48	0.82	0.54	0.39	0.45	0.45	0.45	0.44	0.45	0.45	0.45	0.005
99.54	99.57	99.72	99.80	99.82	99.92	99.80	99.57	99.69	100.05	99.73	100.22	99.77	
0.91	0.40	0.50	0.30	0.53	0.62	0.20	0.23	0.25	0.18	0.10	0.20	0.10	
0.10	0.10	0.10	0.20	0.10	0.30	0.20	0.20	0.20	0.10	0.10	0.20	0.20	
36.50	35.23	33.82	48.15	55.71	66.58	59.44	55.92	54.35	54.83	53.50	59.68	55.39	
12.70	12.73	11.99	21.88	26.78	36.15	27.08	27.22	27.61	27.75	27.16	26.84	27.27	
960	938	932	346	609	156	191	220	213	217	188	188	203	
144	158	144	87	92	80	71	92	76	103	47	98	52	
17	23	23	41	46	46	45	49	52	52	60	55	52	
0	7	0	10	28	131	21	18	19	17	19	15	17	
44	49	54	48	43	53	51	41	42	57	43	53	58	
59	58	60	35	27	24	26	24	26	24	25	27	26	
10	11	10	36	44	154	56	54	76	64	56	51	67	
40	43	42	16	21	12	18	14	20	22	25	16	20	
23	28	13	35	30	43	42	29	37	35	26	29	33	
640	640	660	560	650	550	690	680	690	680	670	690	690	
64	79	52	239	213	250	222	244	230	222	225	222	227	
168	167	170	134	112	105	104	106	107	109	109	110	106	
430	420	450	260	230	180	210	210	210	210	210	220	220	
16.02	15.54	16.31	7.15	8.16	5.38	6.44	6.44	6.38	6.44	6.44	6.38	6.50	
38.41	36.49	37.33	32.23	31.73	21.90	27.78	26.35	25.12	25.01	24.74	26.57	25.64	
15.53	14.10	14.03	22.56	24.26	25.15	26.89	26.81	26.65	25.57	26.30	25.17	26.48	
-	2.60	1.82	0.55	-	1.20	1.41	2.04	3.07	4.14	3.60	3.94	2.96	
5.09	6.16	5.83	10.94	11.99	18.52	11.71	11.68	11.80	12.48	12.10	12.94	11.91	
0.23	-	-	-	1.02	-	-	-	-	-	-	-	-	
11.08	12.26	12.16	13.31	13.16	15.77	12.02	14.60	16.35	16.27	16.37	11.72	15.09	
5.58	4.61	4.71	5.01	4.02	6.24	7.12	5.24	3.95	3.87	3.75	7.10	4.77	
-	-	-	-	-	-	-	-	-	-	-	-	-	
4.20	4.29	4.10	6.15	4.25	4.88	5.39	5.37	5.34	5.26	5.39	5.37	5.39	
3.48	3.60	3.51	1.94	1.28	0.92	1.07	1.07	1.07	1.04	1.07	1.07	1.07	

These compositions are interpreted to represent mixtures of host basalt and melts produced by partial fusion of the granite. The metamorphic xenolith contains small lenses of glass along foliation planes (Table 3). These domains of melt are high in SiO_2 and Al_2O_3, but are clearly different in composition from the granitic glasses and are controlled more by the fusion of phyllosilicates.

Rare-earth-element content

Lavas from the Iskut volcanic field show consistent mantle-normalized *REE* abundance patterns (Fig. 5, Table 4). Relative to primitive mantle, the basalts show 15–30 times enrichment in the light *REE* (*LREE*) and 3–7 times enrichment in the heavy *REE* (*HREE*). The *REE* patterns within and between volcanic centers are

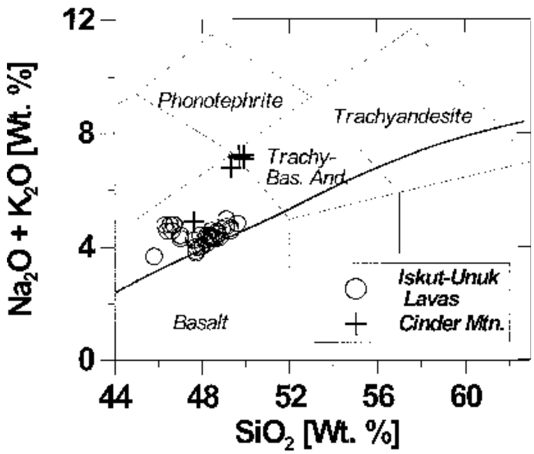

FIG. 2. The compositions of Iskut lavas are plotted as total alkalis *versus* SiO_2 (Le Bas *et al.* 1986). Heavy line represents division between alkaline and subalkaline compositions (Irvine & Baragar 1971). Iskut lavas mainly consist of alkali olivine basalt, except for samples of hawaiite from Cinder Mountain.

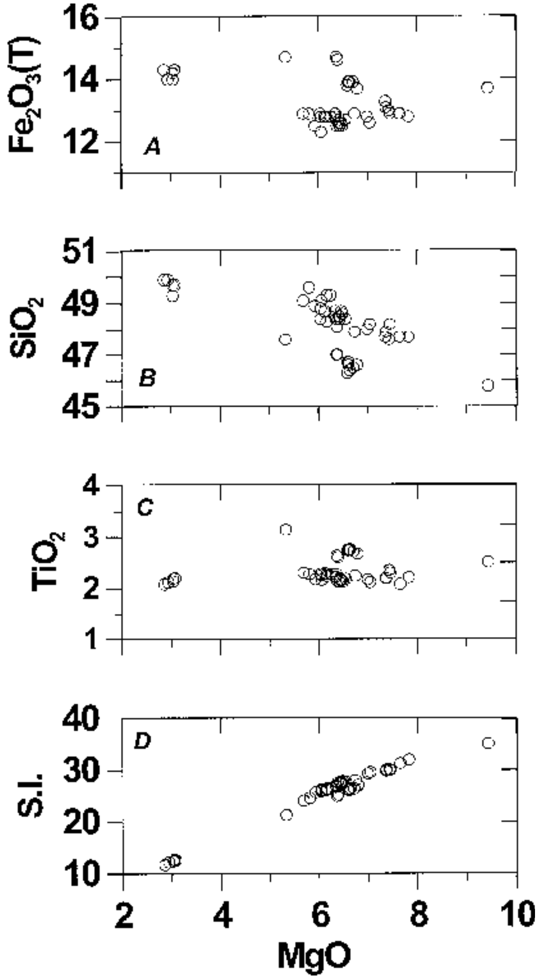

FIG. 3. The chemical compositions of Iskut lavas are shown as (A) Fe_2O_3(T), (B) SiO_2, (C) TiO_2, and Solidification Index (S.I.) plotted against MgO content.

virtually parallel (Fig. 5); values of $[La/Sm]_n$ and $[La/Tb]_n$ for the basalts (Fig. 6) range from 2 to 2.3 and from 6.2 to 7.8, respectively. Hawaiite lavas are two to three times more enriched in *REE* (Fig. 5E) and are slightly more fractionated (Fig. 6). They show similar overall patterns to the basalts (*cf.* Cousens & Bevier 1995), however. The Second Canyon basalt is distinguished from other centers by a slight positive europium anomaly, despite its apparent primitive mineralogical and chemical character (Fig. 5F). This feature is also described in "primitive" Kilauea lavas (Hofmann *et al.* 1984).

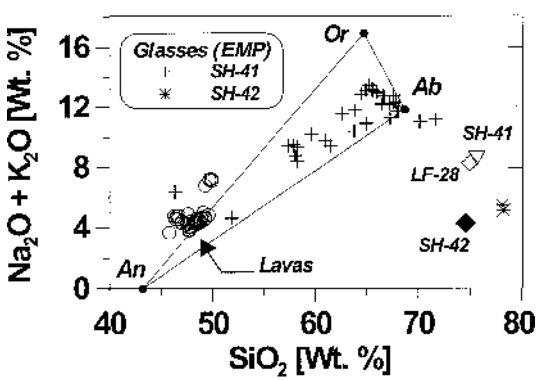

FIG. 4. The compositions of Iskut lavas (circles) are compared to the bulk compositions of partly fused xenoliths (SH–41: granite; SH–42: schist) and a granite (LF–28) that outcrops near Lava Fork. Also plotted are the compositions of glasses from the same partly fused xenoliths (Table 3). The triangular field labeled Or–An–Ab shows the limit of feldspar solid-solutions.

We have also plotted the mantle-normalized *REE* abundance patterns of the partly melted crustal xenoliths recovered from basalts at Lava Fork (Table 4). Both the granitic (SH–41) and metamorphic (SH–42) xenoliths were split and analyzed in duplicate; the duplicate samples show good agreement except in the *HREE* concentrations (Figs. 5G, H). Sample LF–28, from the outcrop of quartz monzonite near the Lava Fork vent, has a substantially different composition than the partly fused granitic xenoliths (Fig. 5G). The xenoliths and monzonite sample show less *REE*-enrichment than do the host

TABLE 3. COMPOSITIONS OF GLASSES (G[1]) AND BULK SAMPLES OF PARTLY- FUSED CRUSTAL XENOLITHS (X[2]), AND A SAMPLE OF LOCAL OUTCROPPING OF PLUTONIC ROCK (P[2])

Label	SH-41								SH-42		SH-41	SH-42	LF-28
Sample	G	G	G	G	G	G	G[3]	G[3]	G	G	X[4]	X[1]	P
SiO_2	57.36	66.03	64.64	67.01	67.00	66.57	63.81	51.85	78.22	78.21	75.70	74.60	76.04
TiO_2	-	-	-	-	-	-	0.56	0.63	0.17	0.13	-	0.36	0.12
Al_2O_3	27.01	18.28	20.19	18.43	19.11	19.53	17.84	26.74	10.36	11.95	13.10	12.60	13.56
FeO_T	0.33	0.15	0.17		0.47	0.40	3.60	3.36	2.12	1.00	0.27	2.50	0.58
MnO	-	-	-	-	-	-	-	-	-	-	-	-	-
MgO	0.34	-	-	-	-	-	1.15	0.48	0.80	0.79	-	0.84	0.11
CaO	4.36	0.67	1.42	0.43	0.50	0.58	2.29	12.35	1.75	1.27	0.68	2.92	0.80
Na_2O	5.10	5.50	6.40	6.31	6.04	6.50	4.42	4.06	3.22	3.99	3.50	3.70	3.78
K_2O	4.35	7.48	6.45	6.99	6.96	6.76	5.97	0.59	1.91	1.47	5.08	0.59	4.55
P_2O_5	0.10	0.27	0.17	0.25	0.13	0.23	0.14	0.26	-	-	0.02	0.06	0.03
Total	98.94	98.38	99.43	99.42	100.21	100.56	99.78	100.30	98.55	98.80	98.35	98.17	99.57

- Indicates elements are at or below detection levels.
[1] Glass compositions determined by electron microprobe at UBC.
[2] Samples analysed by XRF at the GSC , Ottawa (X) and at McGill University (P).
[3] Coloured glasses resulting from mixing of basalt and melted xenolith.
[4] Protoliths to partly fused xenoliths are granitoid (SH-41) and metamorphic schist (SH-42).

TABLE 4. RARE EARTH ELEMENT CONTENTS (PPM) OF SELECTED LAVA SAMPLES FROM THE ISKUT VOLCANIC FIELD

Sample	SH-21	SH-33	SH-39a	SH-39b	IR-8	CG-12	SC-23	KC-22	LF-31	SH-41	SH-42	LF-28[1]	Δ[3]
Rock	Hawaiite	Basalt	Basalt	Basalt	Basalt	Basalt	Basalt	Basalt	Basalt	Xenolith	Xenolith	QM	SH-39
La	63.9	20.3	18.0	17.9	18.4	24.0	19.1	28.0	22.9	9.9	31.2	10.0	0.07
Ce	140.8	46.1	41.0	40.7	40.2	53.9	43.8	61.6	51.8	21.3	58.5	20.0	0.70
Pr	17.5	6.0	5.3	5.4	5.3	7.0	5.8	7.9	6.8	2.6	6.3	2.2	0.05
Nd	72.9	25.6	23.2	23.3	23.1	30.4	25.6	32.2	30.1	10.4	21.9	7.8	0.14
Sm	15.0	6.2	5.5	5.6	5.4	7.1	5.9	7.1	6.6	2.9	3.9	1.6	0.11
Eu	4.79	2.01	1.92	1.94	1.90	2.30	2.80	2.27	2.28	0.27	0.94	0.24	0.02
Gd	14.75	6.21	5.74	5.65	5.78	7.02	6.15	6.89	6.57	2.89	3.41	1.30	0.09
Tb	1.90	0.86	0.81	0.79	0.76	0.93	0.79	0.96	0.89	0.46	0.44	0.18	0.02
Dy	11.03	5.15	4.88	4.82	4.73	5.74	5.89	5.66	5.11	2.69	2.51	0.89	0.06
Ho	2.01	0.96	0.87	0.92	0.87	1.09	0.85	1.08	0.98	0.50	0.47	0.16	0.05
Er	5.33	2.59	2.35	2.39	2.35	2.92	2.26	2.85	2.49	1.41	1.31	0.43	0.04
Tm	0.73	0.37	0.33	0.32	0.32	0.41	0.33	0.42	0.33	0.22	0.20	0.08	0.01
Yb	4.49	2.32	2.10	2.07	1.96	2.61	1.91	2.67	2.11	1.42	1.22	0.49	0.03
Lu	0.63	0.30	0.28	0.28	0.29	0.39	0.27	0.40	0.29	0.20	0.19	0.07	0.00
(La/Sm)[2]	2.76	2.12	2.11	2.06	2.18	2.20	2.10	2.56	2.25	2.20	4.99	4.04	0.05
(La/Yb)[2]	10.22	6.28	6.15	6.21	6.73	6.61	7.16	7.53	7.77	5.14	18.37	14.65	0.06

[1] Sample of outcropping quartz monzonite (analysed by Geological Survey of Canada, Ottawa).
[2] Primitive mantle normalized values (after Sun & McDonough, 1989).
[3] Difference between duplicate analyses of SH-39.

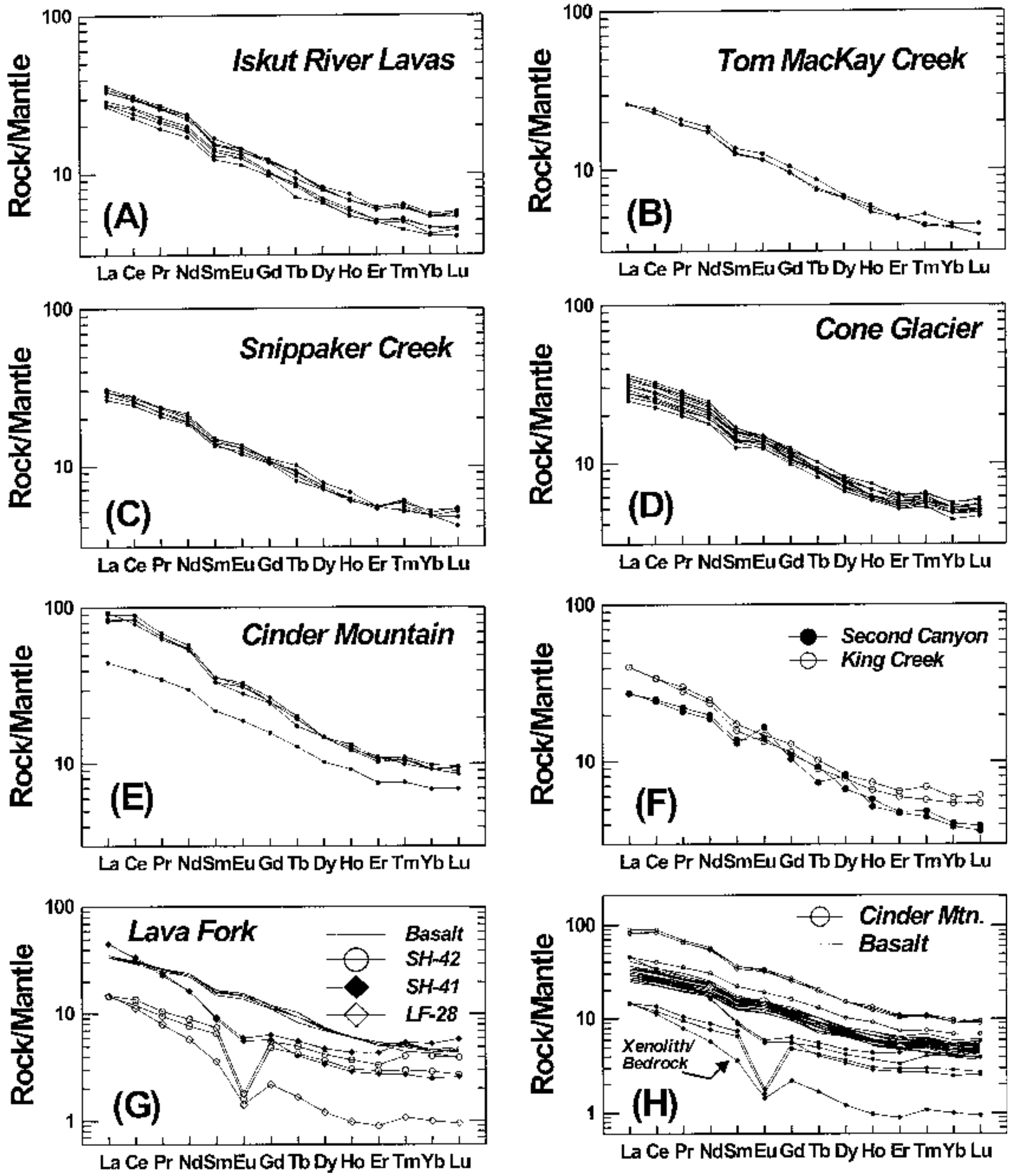

FIG. 5. Rare-earth-element contents of lavas from the Iskut volcanic field are normalized to primitive mantle (REE_n) using data of Sun & McDonough (1989), including samples from: (A) Iskut River, (B) Tom MacKay Creek, (C) Snippaker Creek, (D) Cone Glacier, (E) Cinder Mountain, (F) Second Canyon and King Creek, and (G) Lava Fork. Lava Fork data include compositions of lavas, partly fused crustal xenoliths, and a plutonic bedrock sample (see text). Panel (H) shows all REE_n patterns.

lavas, suggesting that the effects of crustal assimilation may be difficult to discern in terms of *REE* patterns (*e.g.*, Cousens & Bevier 1995, Carignan *et al.* 1994). The monzonite (LF–28) has the lowest *REE* content, whereas the schist (SH–42) has the highest. The fused granite (SH–41) and monzonite show strong negative

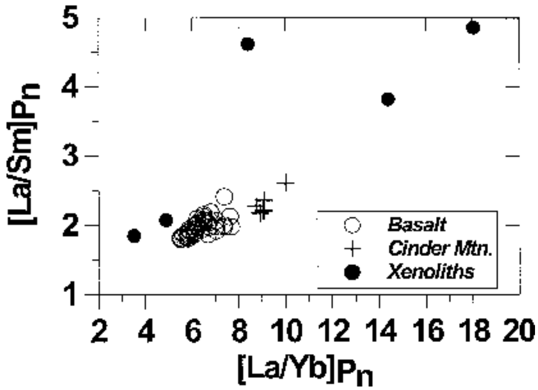

FIG. 6. Light [La/Sm] and total [La/Yb] *REE* fractionation indices for data from Figure 5 and Table 4. The Iskut volcanic rocks show little *REE* fractionation relative to intermediate volcanic rocks from Cinder Mountain. Xenoliths and bedrock samples of granitic rocks show greater *REE* fractionation than do xenoliths of metamorphic rocks.

Eu anomalies, a feature that is not seen in any lavas from the Iskut volcanic field.

MAGMATIC DIFFERENTIATION

The chemical and mineralogical diversity found in these eight volcanic centers is ultimately attributable to differences attending the melting of mantle sources, the transport of the primary magmas through the lithosphere, and the storage and differentiation of the parental magmas. Our strategy to understand their origins is to quantify the possible effects of magmatic differentiation and of assimilation by crustal rocks. The observed assemblages of phenocrysts provide hard evidence for the effects of magmatic differentiation and constrain its character. Assimilation of crustal material is strongly indicated by the abundance of highly fused crustal xenoliths and xenocrysts within many lavas.

Closed versus open systems

We begin with an evaluation of the extent to which the within-center variations in mineralogy and chemical composition can be explained by closed-system processes. Our analysis is restricted to five centers (IR, SNC, CG, CM, LF) for which many flows have been analyzed. We have used element-ratio diagrams (Pearce 1968) to test the phenocryst-sorting hypothesis against the chemical data (*e.g.*, Russell & Nicholls 1988, Nicholls & Russell 1991, Russell & Snyder 1997). The diagram shown in Figure 7 was designed by choosing an appropriate conserved element as the denominator of the ratio, and choosing a set of numerator elements for the *x* and *y* axes that accounts for the target mineral assemblage (Stanley & Russell 1989, Nicholls & Gordon 1994). The target assemblage is defined by the phenocryst assemblage; thus the axes are designed to accommodate olivine ± plagioclase ± augite, although augite is rare. Titanium is used in the denominator because it has low analytical variance (Table 2) and because it is incompatible in these basaltic rocks (Fig. 3). For example, it is geochemically excluded from olivine and plagioclase and occurs only in small amounts (<0.03 atoms per formula unit) in the rare augite megacrysts.

One other consideration affected our design of Figure 7. The numerator coefficients were computed such that the model process (*e.g.*, phenocryst-sorting) will generate a trend with a slope of 1.0. However, we also

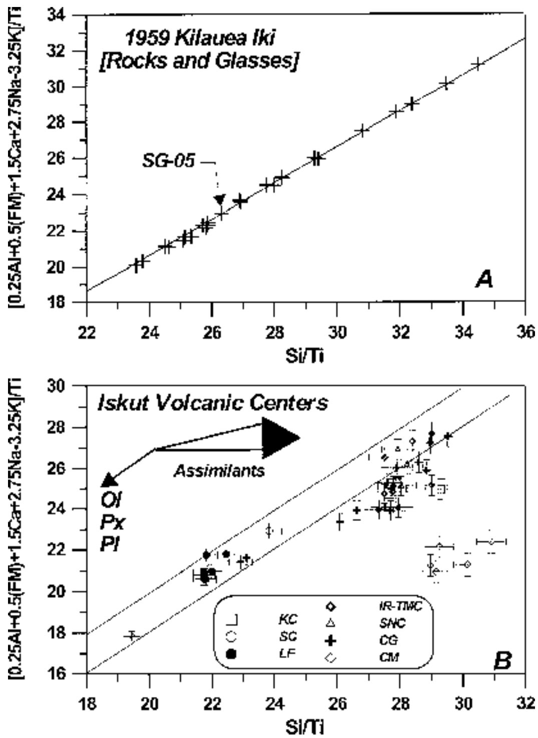

FIG. 7. Element-ratio diagrams designed to test for sorting of olivine ± plagioclase ± augite against the effects of assimilation of crust (*e.g.*, Stanley & Russell 1989). (A) Compositions of basalts from the 1959 eruption of Kilauea Iki are used to calibrate the effects of phenocryst sorting in the absence of assimilation. Model line (m = 1) is drawn through the most magnesian glass composition (SG–05). (B) Lavas from each Iskut volcanic center are plotted in the same compositional space. The data are scattered and, as a group, they fail to define a coherent trend (error bars denote 2σ analytical uncertainties). Inset shows vector representation of effects of crystal sorting *versus* the range of effects due to assimilation of xenoliths and glasses (Table 3, Fig. 4; see Appendix 1).

required that the diagram be sensitive to the addition or loss of granitic components (details are in Appendix 1). In summary, the coefficients used in our axes ensure that lava compositions will plot on a trend with a slope of one if: a) they derive from a single system, b) they have been affected only by fractionation of olivine ± plagioclase ± clinopyroxene, and c) if the system has not gained or lost Ti (Fig. 3). If another mineral is fractionated, or the system is contaminated by crustal material, or the lavas derive from different batches of magma, then the data will depart from the model line.

Compositions of olivine tholeiite lavas from the 1959 eruption of Kilauea Iki (Murata & Richter 1966, Russell & Stanley 1990) are plotted in Figure 7A to demonstrate the effects of phenocryst-sorting in the absence of assimilation. These lavas contain abundant phenocrysts of olivine and small amounts of clinopyroxene and plagioclase. The model hypothesis is represented by a line with a slope of 1.0 drawn through the most magnesian glass composition reported (SG–05; *cf.* Russell & Stanley 1990). All compositions lie directly on, or within analytical error of, the model line.

The compositions of lavas from the Iskut volcanic field contrast greatly with the compositional data from Kilauea (Fig. 7B), as they show scatter that clearly exceeds analytical uncertainties. Two model lines (m = 1) are drawn through a Lava Fork sample and an Iskut River sample, but the data fail to define a parallel compositional trend. Even by excluding the CM hawaiites, these volcanic rocks record chemical variations that cannot be attributed to simple sorting of the observed assemblage of phenocrysts.

The above result is to be expected because the data shown on Figure 7B derive from eight separate volcanic centers. Data for five of the volcanic centers are plotted individually in Figure 8, and model lines representing closed-system processes are drawn through the least-fractionated sample for each suite. This sample was identified on the basis of MgO content, composition of olivine phenocrysts, and solidification index. None of the individual suites of lavas (IR, Fig. 8A; SNC, Fig. 8B; CG, Fig. 8C; CM, Fig. 8D) can be related to a single magma by sorting of olivine ± plagioclase ± augite. Lavas from Lava Fork have a range of compositions that is only slightly greater than the limits of analytical uncertainty (Fig. 8E). In most centers, the trend generated by the lavas is nearly perpendicular to the model trend for crystal sorting. This is a clear indication of the involvement of an open-system process.

Mass-Balance Models

Hypothesis

Crustal xenoliths are common in at least five of the eight Iskut volcanic centers. Complexly zoned, sieved-textured plagioclase phenocrysts, which may represent surviving and cannibalized xenocrysts of plagioclase from crustal sources (*e.g.*, Tsuchiyama 1985), are also pervasive and abundant within the basalt lavas. Such textures in phenocrysts are particularly common in basalts that have been influenced by assimilation processes (*e.g.*, Harris & Bell 1982) or magma mixing (*e.g.*, Wilcox 1954, Kuo & Kirkpatrick 1982).

Styles of assimilation can vary from bulk assimilation to selective assimilation (assimilation of partial melts) and depend on the length and time scales of magma–host interaction (*e.g.*, Watson 1982, Huppert & Sparks 1985, Grove *et al.* 1982, Russell *et al.* 1995, Edwards & Russell 1998). Many xenoliths in the Iskut

TABLE 5. RESULTS FROM MASS BALANCE MODELLING OF FRACTIONATION AND ASSIMILATION PROCESSES

Input Parameters					Model Results				
Center	Parent	Daughter	Ol (Fo %)	Pl (An %)	Ol (g)	PL (g)	Assimilant (g)[1]	SSQ[2]	α[3]
IR	IR-8	IR-6	73.4	58.5	3.90	7.53	-4.14	0.50	< 0.001
SNC	SH-34	SH-01	74.9	60.5	2.70	1.84	-2.50	0.41	< 0.001
CG	SH-14	SH-13	80.3	50.6	5.10	9.71	-7.08	0.70	0.002
CG to CM	SH-14	CM-20	80.3	50.6	15.59	39.18	-18.10	7.9	0.64
CM	CM-20	CM-21	52.6	42.3	0.12	0.18	-1.94	0.02	< 0.001
SC - CG[4]	SC-23	SH-14	82.0	69.3	1.30	-6.08	-	4.3	0.17
SC - CG	SC-23	SH-14	82.0	69.3	1.04	-5.20	-2.06	3.0	0.11

[1] Modal composition of glass from SH-41: SiO_2 (66.9), Al_2O_3 (18.8), FeO (0.3), CaO (0.5), Na_2O (6.4), K_2O (7.1).
[2] Solutions obtained by χ^2 minimization methods (see text); sums of residuals squared (SSQ) are reported for comparisons with literature.
[3] Tolerance (α) denotes probability of getting observed value of SSQ by chance even when model is correct.
[4] Solution for model that considers only sorting of olivine and plagioclase (see text).

lavas are partly fused, digested or reacted, and their presence lends strong support for a selective style of assimilation whereby elements residing in the earlier melting phases are preferentially incorporated into the host magma by melt diffusion or blending of melts (*e.g.*, Patchett 1980, Watson 1982, Watson & Jurewicz 1984, Beard *et al.* 1993). Consequently, we suggest that the effective contaminant, produced by assimilation of crustal rocks, must lie within the compositional field of glass compositions found in the partly fused xenoliths described above (Table 3, Fig. 4).

Table 5 contains expressions of the crystal fractionation – assimilation hypotheses proposed for the four centers within the Iskut volcanic field that show significant chemical variation. Below, we develop a mass-balance strategy to test whether the compositions of lavas

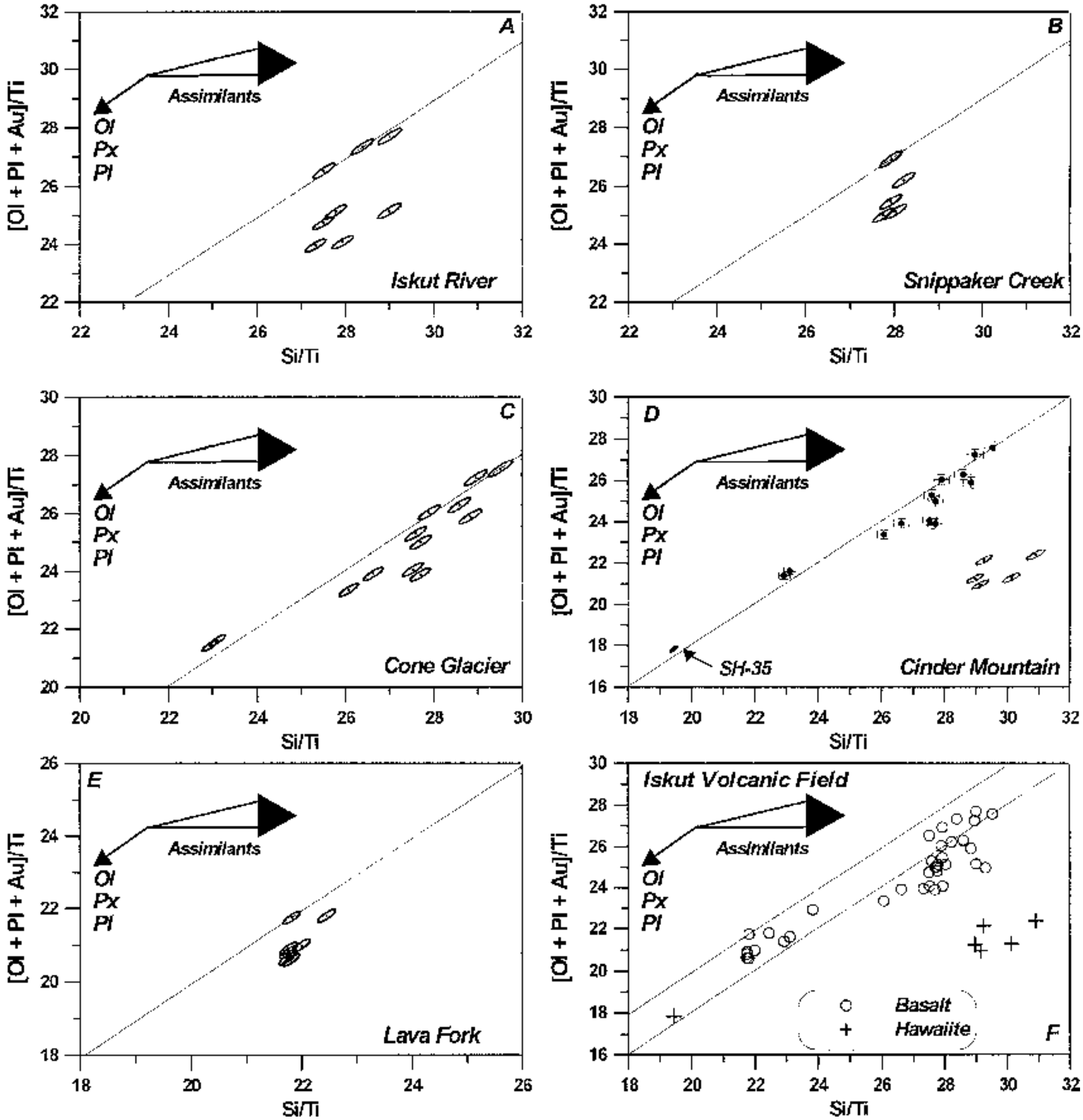

FIG. 8. Chemical compositions of lavas from individual volcanic centers plotted in (olivine ± plagioclase ± augite)-sorting diagrams used in Figure 7. Ellipses denote 1σ errors due to analytical uncertainties. Datasets include: (A) Iskut River, (B) Snippaker Creek, (C) Cone Glacier, (D) Cinder Mountain, (E) Lava Fork, and (F) all data together.

from a single center record the effects of both crystal sorting and crustal assimilation. Our solutions to these models provide bounds on the relative importance of these two processes. In each case, the compositions of olivine and plagioclase used in the modeling are measured compositions of cores to phenocrysts from the actual samples. We have used an average glass composition as a proxy for the assimilant; specifically, we used the modal composition of the colorless glass compositions from sample SH–41.

Model

For each oxide (*n* in total), there is a linear equation ensuring mass balance between the initial and final system:

$$\sum_{j=1}^{m} X_j \left[s_{i,j} - \frac{wd_i}{100} \right] = \left[wp_i - wd_i \right] \quad (1)$$

where $\mathbf{wp}_i$ and $\mathbf{wd}_i$ are the wt.% concentrations of the i^{th} oxide in the parent and derivative rock, respectively. The form of Eq. 1 is taken from Stout & Nicholls (1977) and has the attribute that the mass-balance solutions are less sensitive to the absolute abundances of each oxide and more sensitive to the differences between parent and derivative samples. The variable $\mathbf{s}_{i,j}$ is the weight fraction of oxide i in the phase j. The *m* variables $\mathbf{X}_j$ are the unknown masses of phases added or subtracted to the parent magma. Solving this overdetermined ($n > m$) system of linear equations returns estimates of $\mathbf{X}_j$.

Armed with reliable estimates of measurement errors (σ_i ; see Table 2), we can move from a "best- fit" least-squares analysis approach, to a mapping of "confidence limits" on the optimal solution using conventional methods reviewed by Press *et al*. (1986). This requires minimization of the χ^2 function:

$$\chi^2 = \sum_{i=1}^{n} \left[\frac{y_i - \hat{A}(X_1, X_2, \ldots X_m)}{\sigma_i} \right]^2 \quad (2)$$

where $\mathbf{y}_i$ are the measured values, $\hat{\mathbf{A}}(\mathbf{X})$ are the values predicted by the model, and the summation is over the *n* oxide-equations. Minimization of this function nominally returns the "weighted least-squares" solution.

There are two differences in our approach to mass-balance modeling relative to others. First, we compare the value of the minimized function (χ^2_{model}) directly against the χ^2 distribution for *n–m* degrees of freedom (Press *et al.* 1986) as a means of assessing the goodness of fit (α; Table 5). Specifically, the values of α recorded in Table 5 represent the probabilities of obtaining the observed χ^2_{model} value by chance, or of rejecting the fractionation–assimilation hypothesis where it is, in fact, true. Where the χ^2_{model} values are small relative to the analytical errors, we can expect a small value of α and be confident ($1 - \alpha$) that the model is consistent with, or permitted by, the data. Of course, this does not preclude the existence of an equally valid alternative explanation. In situations where the χ^2_{model} values are large relative to the analytical uncertainties, values of α will increase substantially. This case indicates that there is a high probability of obtaining the observed χ^2_{model} value simply by chance, that we cannot assign a high degree of confidence ($1 - \alpha$) to the hypothesis, and that we may reject it. This strategy of comparing values χ^2_{model} to the χ^2 distribution circumvents the use of arbitrary values of sums of squares (*e.g.*, SSQ = 1) to decide whether to accept or reject a particular mass-balance model.

A second difference is that, rather than consider a single solution that happens to coincide with the minimum SSQ, we have elected to use the χ^2 distribution to create confidence limits (*e.g.*, 95%) on the solution. This approach has several merits. Firstly, we are able to set *a priori* the confidence limits that we wish to use, and then map the range of all possible solutions that are permitted under these limits. Given that we accept the model (low values of α), this map shows the range of all solutions that must be considered as being equally valid. For example, the solution space may enclose zero amounts of a phase, which would indicate that the phase may not be involved. Secondly, the two-dimensional (2–D) projections of the solution space show correlations among model parameters that are critical in terms of interpreting the ranges of acceptable values.

RESULTS

Figure 9 shows the solutions to the mass-balance problems posed in Table 5 for the IR, SNC, CG and CM volcanic centers. The solutions are expressed as 68, 95 and 99% confidence ellipses and are shown as 2–D projections containing the point associated with the minimum χ^2 value (the center). The projections show the complete range of masses of olivine, plagioclase and assimilant (per 100 g of magma) consistent with the compositional difference between parent and daughter composition.

In the case of lavas from Iskut River, Snippaker Creek, and Cone Glacier, the solutions require the fractionation of positive amounts of both olivine and plagioclase and the assimilation (negative) of crustal material (Table 5). All three phases are required to explain the observed compositional differences because the confidence limits fail to include the zero axis for any phase. The hawaiite lavas from Cinder Mountain record a slightly different process (Fig. 9, Table 5). At the 95% confidence limit, the optimal solution for Cinder Mountain hawaiite requires assimilation of 1.9 ± 0.6 g of granitic melt (Table 5). However, the solution permits gains or losses of small amounts of olivine and plagioclase (Fig. 9). More importantly, the mass-balance

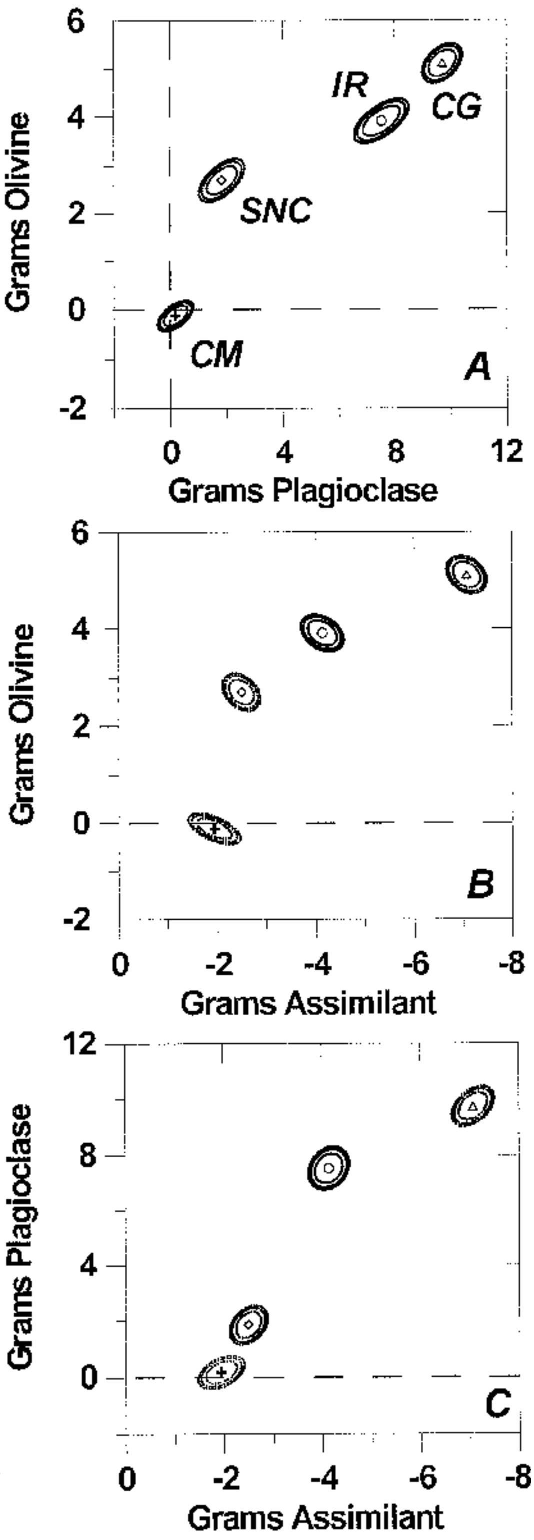

FIG. 9. Graphical representation of results of mass-balance modeling from Table 5. Optimal solutions are shown as 68, 95 and 99% confidence limits on masses (g) of olivine and plagioclase fractionated (positive) and assimilant added (negative) per 100 g of original magma. Solutions for Iskut River, Snippaker Creek, Cone Glacier, and Cinder Mountain centers are considered acceptable (Table 5), and all require assimilation of crustal rocks.

model suggests that chemical variations within the hawaiites can be explained by assimilation alone; the 95% confidence limit solution-space includes the zero axis for fractionation of both olivine and plagioclase.

We also tested whether the CM hawaiite could be derived from the Cone Glacier basalt by fractionation and assimilation (Table 5). The mass-balance modeling showed this process to be unreasonable because it requires an extraordinary amount of crystallization (55%), the sums of squares of residuals are exceedingly high, and the corresponding confidence level ($1 - \alpha$) is low (Table 5). Thus although we have an adequate explanation for chemical diversity within the hawaiite suite, their ultimate origins remain enigmatic. Past explanations for hawaiite in the Canadian Cordillera include fractional crystallization (Souther & Hickson 1984, Cousens & Bevier 1995), and assimilation or assimilation and crystallization (*e.g.,* Stout & Nicholls 1983, Charland *et al.* 1993).

DISCUSSION

Figure 10 provides a direct comparison between the mass of assimilant *versus* the total mass of crystals fractionated. In each case, the calculations require that the masses of crystals fractionated exceed the masses assimilated. For the Iskut volcanic field, the ratio of assimilation to fractionation is approximately 1:2 (Fig. 10). This finding compares well to the results of Stout & Nicholls (1983), who modeled the origin of hawaiite from the Itcha Mountain Range in terms of coupled crystallization and assimilation. On the basis of thermodynamic and mass-balance calculations they showed that, for assimilation-to-crystallization ratios up to 1:2, the sensible and latent heats suffice to support the process. Conversely, at higher ratios of assimilation to crystallization (*e.g.,* 1:1), an external source of heat is required. Furthermore, Edwards & Russell (1998) showed that model paths of isenthalpic assimilation – fractional crystallization processes converge to ratios of 1:2 (*e.g.,* r values of 0.5; DePaolo 1981). Thus our mass-balance solutions for lavas within the Iskut volcanic field (*e.g.,* 1:2 ratio of assimilation to crystallization) also appear to be energetically feasible (Stout & Nicholls 1983, Edwards & Russell 1998).

Our last calculation is aimed at elucidating the petrogenetic relationship between these lavas and potential primary magmas. The Second Canyon basalt is the most

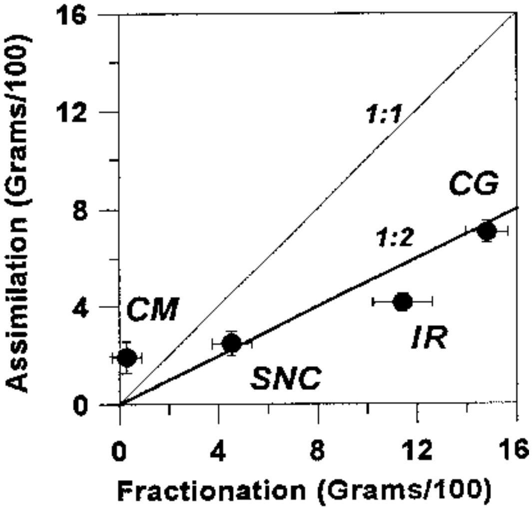

FIG. 10. Results of mass-balance modeling summarized as total mass of fractionated material *versus* mass of assimilated material. Error bars represent the 2σ uncertainties on the model solutions. Reference lines show fixed ratios of fractionated to assimilated masses. Centers from the Iskut volcanic field describe a 1:2 relationship between assimilation and crystallization (see text).

primitive lava in the region (MgO: 9.25 wt.%, S.I. 36, normative *ne*). Mineralogically, the lava contains phenocrysts of olivine ($Fo_{84–82}$) and plagioclase (An_{69}); obvious xenocrystic or megacrystic plagioclase is absent. Using the olivine–liquid thermodynamic model of Roeder & Emslie (1970), the predicted olivine-saturation conditions for a melt of this chemical composition are $Fo_{87–83}$ and 1244–1252°C, depending on the assumed ratio of Fe^{2+} to Fe^{3+}.

We have used the composition of the Second Canyon basalt (SC–23) as a proxy for the composition of a likely primary magma to the Iskut volcanic field. Clearly, this is an approximation. We have then investigated the potential mass-balance relationships between this magma and the least-evolved lava from Cone Glacier (SH–14). We tested two separate hypotheses concerning these two magma compositions: i) sorting of olivine and plagioclase, and ii) sorting of olivine and plagioclase coupled to assimilation of crustal material (Table 5, Fig. 11). The closed system process requires fractionation of small amounts of olivine (1.3 g) and substantial accumulation of plagioclase (6 g) (Fig. 11A). The solution has residual sums of squares (Table 5) that are larger than associated with other models (4.3) and large enough to reject the hypothesis (*e.g.,* Stout & Nicholls 1983).

The solution for the crystal-sorting-and-assimilation hypothesis (Figs. 11A, B, C) requires fractionation of small amounts of olivine (1 g) and accumulation of substantial amounts of plagioclase (–5 g), but also involves assimilation of 2 g of crustal material. The sums of squares of residuals are reduced to 3 because of the extra fit parameter (Table 5). However, the value of α (in which the additional fit parameter is already accounted for) is also substantially reduced (0.17 to 0.11) and, therefore, the model must be considered as close to acceptable (*e.g.,* Stout & Nicholls 1983) on the basis of the corresponding confidence level (0.89). Lastly, the 95% confidence limits on the solution (Fig. 11) do not enclose the zero axis for any of the phases, indicating that all three phases are required. The projected confidence ellipses (Fig. 11) also provide insights into the nature of correlations between the model parameters. Note that the mass of assimilant is virtually independent of the masses of olivine and plagioclase. The role of assimilation cannot be subsumed simply by changing the amounts or proportions of the fractionated solids.

This last computation suggests that, relative to Second Canyon basalt, the Cone Glacier lavas have accumulated substantial plagioclase and assimilated granitic crust, whilst crystallizing only a minor proportion of olivine. One implication of this inference is that the large vitreous-looking plagioclase crystals in the Cone Glacier lavas are cognate; their abundance is a result of crystal accumulation. Indeed, the abundant and pervasive large plagioclase phenocrysts that characterize lavas within the Iskut volcanic field may be a direct result of crustal assimilation. Assimilation of feldspar can greatly increase the stability field of plagioclase in basaltic liquids, with the consequence that plagioclase crystallizes earlier and in greater quantities (*e.g.,* Bowen 1928, Edwards & Russell 1998).

CONCLUSIONS

The effects and importance of crustal assimilation on Quaternary magmatism in the Canadian Cordillera have been alluded to by many past investigators (*e.g.,* Stout & Nicholls 1983, Souther & Hickson 1984, Eiché *et al.* 1987, Carignan *et al.* 1994, Cousens & Bevier 1995, Edwards & Russell 1999), but have not been examined quantitatively except in a few cases (*e.g.,* Souther & Hickson 1984, Stout & Nicholls 1983). In our experience, the traditional reliance on isotopes and trace elements to recognize and quantify crustal assimilation (*e.g.,* Carter *et al.* 1978, DePaolo 1981, Samson *et al.* 1989, Brandon *et al.* 1993, Carignan *et al.* 1994) may be somewhat misplaced in the northern Canadian Cordillera. These tools tend to be blunted by the nature of the underlying lithosphere (*e.g.,* Samson *et al.* 1989, Cousens & Bevier 1995, Carignan *et al.* 1994, Edwards & Russell 2000). For example, many of the arc-derived rocks that dominate Stikinia and serve as basement to the NCVP are, in terms of isotopic and trace-element compositions, indistinguishable from the NCVP volcanic rocks and some modern-day OIB (*e.g.,* Carignan *et* *al.* 1994, Cousens & Bevier 1995, Edwards & Russell 2000). Detecting the effects of crustal contamination using these data alone is problematic at best.

Quaternary lavas from the Iskut volcanic field have within-center compositional variations that cannot be accounted for by simple sorting of the phenocryst assemblage (olivine and plagioclase) or even cryptic fractionation of higher-pressure pyroxene (found as rare partly resorbed megacrysts). The textural, mineralogical and whole-rock chemical data suggest that assimilation of crustal material has played a significant role in the petrogenesis of the lavas in the Iskut volcanic field. Mass-balance modeling of the major-element data provides a quantitative estimate (1:2) of the proportions of material assimilated *versus* fractionated. We suggest that assimilation of crustal material may be more widespread in the NCVP than is currently recognized. One of the ultimate goals of petrologists is to map physical and chemical variations in the mantle underlying the Canadian Cordillera. In order to achieve this end, it is critical that we continue to recognize and quantify the effects of assimilation, so that source-region variations can be more clearly revealed.

Acknowledgements

It is our privilege to contribute this manuscript to the volume dedicated to the illustrious career of Peter Roeder. We thank Dante Canil for the original invitation and Bob Martin for his editorial support. Field work costs associated with this research were borne by the Geological Survey of Canada; we are indebted to R.G. Anderson for this support. We also acknowledge financial support from the Natural Sciences and Engineering Research Council *via* a research grant to JKR. Ideas and arguments advanced in this paper have benefitted from conversations shared with Jim Nicholls, Ben Edwards and Bob Anderson. The review process involving A.D. Fowler and M. Garcia provided a basis for improving the clarity and consistency of the manuscript.

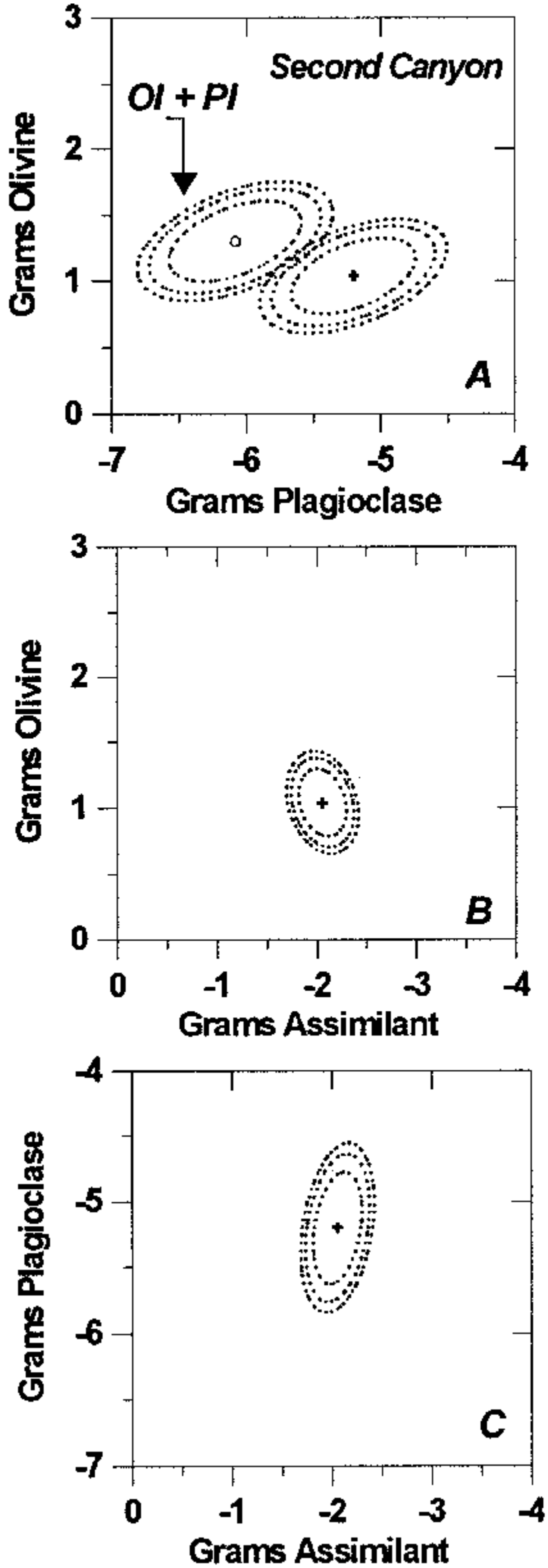

FIG. 11. The mass-balance relationships between a "close-to-primitive" basalt composition from the Iskut volcanic field (Second Canyon) and a "parental" lava composition from the Cone Glacier volcanic field (see text and Table 5). Panel (A) shows solutions for both: i) sorting of olivine and plagioclase, and ii) sorting of olivine and plagioclase and assimilation of crustal material.

References

Al-Rawi, Y. & Carmichael, I.S.E. (1967): A note on the natural fusion of granite. *Am. Mineral.* **52**, 1806-1814.

Anderson, R.G. (1993): A Mesozoic stratigraphic and plutonic framework for northwestern Stikinia (Iskut River area), northwestern British Columbia, Canada. *In* Mesozoic Paleogeography of the Western United States II (G.C. Dunne & K.A. McDougall, eds.). *Soc. Econ. Paleontol. Mineral.* (*Pacific Sect.*) **71**, 477-494.

Beard, J.S., Abitz, R.J. & Lofgren, G.E. (1993): Experimental melting of crustal xenoliths from Kilbourne Hole, New Mexico and implications for the contamination and genesis of magmas. *Contrib. Mineral. Petrol*. **115**, 88-102.

Bevier, M.L. (1992): A dominant asthenospheric mantle source for Late Miocene – Quaternary volcanic rocks, Stikine Volcanic Belt, British Columbia and Yukon Territory, Canada. *Trans. Am. Geophys. Union* (*Eos*) **73**, 334 (abstr.).

Bowen, N.L. (1928): *The Evolution of the Igneous Rocks*. Princeton University Press, Princeton, New Jersey.

Brandon, A.D., Hooper, P.R., Goles, G.G. & Lambert, R.St.J. (1993): Evaluating crustal contamination in continental basalts: the isotopic compositions of the Picture Gorge basalt of the Columbia River basalt group. *Contrib. Mineral. Petrol*. **114**, 452-464.

Britton, J.M., Fletcher, B.A. & Alldrick, D.J. (1989): Snippaker map area (104B/6E, 7W, 10W, 11E). *In* Geological Fieldwork 1989. *B.C. Ministry of Energy, Mines and Petrol. Resources, Pap*. **1990-1**, 115-125.

________, Webster, L.C.L. & Alldrick, D.J. (1988): Unuk map area (104B/7E, 8W, 9W, 10E). *In* Geological Fieldwork 1988. *B.C. Ministry of Energy, Mines and Petrol. Resources, Pap.* **1989-1**, 241-250.

Carignan, J., Ludden, J. & Francis, D. (1994): Isotopic characteristics of mantle sources for Quaternary continental alkaline magmas in the northern Canadian cordillera. *Earth Planet. Sci. Lett*. **128**, 271-286.

Carter, S.R., Evensen, N.M., Hamilton, P.J. & O'Nions, R.K. (1978): Neodymium and strontium isotope evidence for crustal contamination of continental volcanics. *Science* **202**, 743-747.

Charland, A, Francis, D. & Ludden, J. (1993): Stratigraphy and geochemistry of the Itcha Volcanic Complex, central British Columbia. *Can. J. Earth Sci*. **30**, 132-144.

Cousens, B.L. & Bevier, M.L. (1995): Discerning asthenospheric, lithospheric, and crustal influences on the geochemistry of Quaternary basalts from the Iskut–Unuk rivers area, northwestern British Columbia. *Can. J. Earth Sci*. **32**, 1451-1461.

Cui, Y. & Russell, J. K. (1995): Magmatic origins of calc-alkaline intrusions from the Coast Plutonic Complex, southwestern British Columbia. *Can. J. Earth Sci.* **32**, 1643-1667.

DePaolo, D.J. (1981): Trace element and isotopic effects of combined wallrock assimilation and fractional crystallization. *Earth Planet. Sci. Lett.* **53**, 189-202.

Edwards, B.R. (1997): *Field, Kinetic and Thermodynamic Studies of Magmatic Assimilation in the Northern Cordilleran Volcanic Province, Northwestern British Columbia*. Ph.D. thesis, Univ. of British Columbia, Vancouver, British Columbia.

________ & Russell, J.K. (1994): Preliminary stratigraphy of Hoodoo Mountain volcanic centre, northwestern British Columbia. *Geol. Surv. Can., Current Res.* **1994-A**, 69-76.

________ & ________ (1998): Time scales of magmatic processes: new insights from dynamic models for magmatic assimilation. *Geology* **26**, 1103-1106.

________ & ________ (1999): Northern Cordilleran volcanic province: a northern Basin and Range? *Geology* **27**, 243-246.

________ & ________ (2000): Distribution, nature and origin of Neogene–Quaternary magmatism in the Northern Cordilleran volcanic province, Canada. *Geol. Soc. Am., Bull*. **112**, 1280-1295.

Eiché, G.E., Francis, D.M. & Ludden, J.N. (1987): Primary alkaline magmas associated with the Quaternary Alligator Lake volcanic complex, Yukon Territory, Canada. *Contrib. Mineral. Petrol.* **95**, 191-201.

Elliott, R.L., Koch, R.D. & Robinson, S.W. (1981): Age of basalt flows in the Blue River Valley, Bradfield Canal Quadrangle. *In* the U.S. Geological Survey of Alaska, Accomplishments during 1979. *U.S. Geol. Surv., Circ.* **823-B**, B115-B116.

Francis, D. & Ludden, J. (1990): The mantle source for olivine nephelinite, basanite and alkaline olivine basalt at Fort Selkirk, Yukon, Canada. *J. Petrol.* **31**, 371-400.

Gabrielse, H. & Yorath, C.J. (1991): Tectonic synthesis. *In* Geology of the Cordilleran Orogen in Canada (H. Gabrielse & C.J. Yorath, eds.). *Geol. Surv. Can., Geology of Canada* **4**, 677-705.

Glazner, A.F. & Farmer, G.L. (1992): Production of isotopic variability in continental basalts by cryptic crustal contamination. *Science* **255**, 72-74.

Grove, E.W. (1974): Deglaciation – a possible triggering mechanism for Recent volcanism. *International Association of Volcanology and Chemistry of the Earth's Interior, Proc. Symp. on Andean and Antarctic Volcanology Problems* (*Santiago*), 88-97.

________ (1986): Geology and mineral deposits of the Unuk River – Salmon River – Anyox area. *B.C. Ministry of Energy, Mines and Petrol. Resources, Bull.* **63**.

GROVE, T.L., GERLACH, D.C. & SANDO, T.W. (1982): Origin of calc-alkaline series lavas at Medicine Lake volcano by fractionation, assimilation and mixing. *Contrib. Mineral. Petrol.* **80**, 160-182.

HARRIS, C. & BELL, J.D. (1982): Natural partial melting of syenite blocks from Ascension Island. *Contrib. Mineral. Petrol.* **79**, 107-113.

HAUKSDÓTTIR, S., ENEGREN, E.G. & RUSSELL, J.K. (1994): Recent basaltic volcanism in the Iskut–Unuk rivers area, northwestern British Columbia. *Geol. Surv. Can., Current Res.* **1994-A**, 57-67.

HOFMANN, A.W., FEIGENSON, M.D. & RACZEK, I. (1984): Case studies on the origin of basalt. III. Petrogenesis of the Mauna Ulu eruption, Kilauea, 1969–1971. *Contrib. Mineral. Petrol.* **88**, 24-35.

HUPPERT, H.E. & SPARKS, R.S.J. (1985): Cooling and contamination of mafic and ultramafic magmas during ascent through continental crust. *Earth Planet. Sci. Lett.* **74**, 371-386.

IRVINE, T.N. & BARAGAR, W.R.A. (1971): A guide to the chemical classification of the common volcanic rocks. *Can. J. Earth Sci.* **8**, 523-548.

JENNER, G. A., LONGERICH, H. P., JACKSON, S. E. & FRYER, B. J. (1990): ICP–MS: a powerful tool for high-precision trace-element analysis in earth sciences: evidence from analysis of selected U.S.G.S. reference samples. *Chem. Geol.* **83**, 133-148.

KACZOR, S.M., HANSON, G.N. & PETERMAN, Z.E. (1988): Disequilibrium melting of granite at the contact with a basic plug: a geochemical and petrographical study. *J. Geol.* **96**, 61-78.

KERR, A. (1948): Lower Stikine and western Iskut River areas, British Columbia. *Geol. Surv. Can., Mem.* **246**.

KUO, CHUAN-LUNG & KIRKPATRICK, R.J. (1982): Pre-eruption history of phyric basalts from DSDP Legs 45 and 46; evidence from morphology and zoning patterns in plagioclase. *Contrib. Mineral. Petrol.* **79**, 13-27.

KUSHIRO, I. (1960): Si–Al relation in clinopyroxenes from igneous rocks. *Am. J. Sci.* **258**, 548-554.

LE BAS, M.J. (1962): The role of aluminum in igneous clinopyroxenes with relation to their parentage. *Am. J. Sci.* **260**, 267-288.

________, LE MAITRE, R.W., STRECKEISEN, A. & ZANETTIN, B. (1986): A chemical classification of volcanic rocks based on the total alkali – silica diagram. *J. Petrol.* **27**, 745-750.

LE MAITRE, R.W. (1974): Partially fused granite blocks from Mt. Elephant, Victoria, Australia. *J. Petrol.* **15**, 403-412.

MAURY, R.C. & BIZOUARD, H. (1974): Melting of acid xenoliths into a basanite: an approach to the possible mechanisms of crustal contamination. *Contrib. Mineral. Petrol.* **48**, 275-286.

MONGER, J.W.H. (1984): Cordilleran tectonics: a Canadian perspective. *Soc. Géol. Fr., Bull.* **26**, 255-278.

MOORE, J.G., HICKSON, C.J. & CALK, L. (1995): Tholeiitic–alkalic transition at subglacial volcanoes, Tuya region, British Columbia, Canada. *J. Geophys. Res.* **100**, 24,577-24,592.

MURATA, K.J. & RICHTER, D.H. (1966): Chemistry of the lavas of the 1959–1960 eruption of Kilauea volcano. *U.S. Geol. Surv., Prof. Pap.* **537-A**.

NICHOLLS, J. & GORDON, T.M. (1994): Procedures for the calculation of axial ratios on Pearce element-ratio diagrams. *Can. Mineral.* **32**, 969-977.

________ & RUSSELL, J.K. (1991): Major-element chemical discrimination of magma-batches in lavas from Kilauea volcano, Hawaii, 1954–1971 eruptions. *Can. Mineral.* **29**, 981-993.

PATCHETT, P.J. (1980): Thermal effects of basalt on continental crust and crustal contamination of magmas. *Nature* **283**, 559-561.

PEARCE, T.H. (1968): A contribution to the theory of variation diagrams. *Contrib. Mineral. Petrol.* **19**, 142-157.

PRESS W.H., FLANNERY, B.P., TEUKOLSKY, S.A. & VETTERLING, W.T. (1986): *Numerical Recipes: The Art of Scientific Computing.* Cambridge University Press, Cambridge, U.K.

READ, P.B., BROWN, R.L., PSUTKA, J.F., MOORE, J.M., JOURNEAY, M., LANE, L.S. & ORCHARD, M.J. (1989): Geology of parts of Snippaker Creek (104B/10), Forrest Kerr Creek (104B/15), Bob Quinn Lake (104B/16), Iskut River (104G/1) and More Creek (104G/2). *Geol. Surv. Can., Open File* **2094**.

ROEDER, P.L. & EMSLIE, R.F. (1970): Olivine–liquid equilibrium. *Contrib. Mineral. Petrol.* **29**, 275- 289.

RUSSELL J.K., EDWARDS, B.R. & SNYDER, L.D. (1995): Volatile production possibilities during magmatic assimilation: heat and mass-balance constraints. *In* Magmas, Fluids and Ore Deposits (J.F.H. Thompson, ed.). *Mineral. Assoc. Can., Short Course* **23**, 1-24.

________ & NICHOLLS, J. (1988): Analysis of petrologic hypotheses with Pearce element ratios. *Contrib. Mineral. Petrol.* **99**, 25-35.

________, ________, STANLEY, C.R. & PEARCE, T.H. (1990): Pearce element ratios – a paradigm for the testing of petrologic hypotheses. *Trans. Am. Geophys. Union* (*Eos*) **71**, 234-236, 246-247.

________ & SNYDER, L.D. (1997). Petrology of picritic basalts from Kamloops, British Columbia: primary liquids from a Triassic–Jurassic arc. *Can. Mineral.* **35**, 521-541.

________ & STANLEY, C.R. (1990): Origins of the 1954–1960 lavas, Kilauea Volcano, Hawaii: major element constraints on shallow reservoir magmatic processes. *J. Geophys. Res.* **95**, 5021-5047.

SAMSON, S.D., MCCLELLAND, W.C., PATCHETT, P.J., GEHRELS, G.E. & ANDERSON, R.G. (1989): Evidence from neodymium isotopes for mantle contributions to Phanerozoic crustal genesis in the Canadian Cordillera. *Nature* **337**, 705-709.

SIGURDSSON, H. (1968): Petrology of acid xenoliths from Surtsey. *Geol. Mag.* **105**, 440-453.

SOUTHER, J.G. (1990a): Volcano tectonics of Canada. *In* Volcanoes of North America, United States and Canada (C.A. Wood & J. Kienle, eds.). Cambridge University Press, Cambridge, U.K. (111-116).

________ (1990b): Iskut–Unuk River cones, Canada. *In* Volcanoes of North America, United States and Canada (C.A. Wood & J. Kienle, eds.). Cambridge University Press, Cambridge, U.K. (128-129).

________ (1992): The late Cenozoic Mount Edziza volcanic complex, British Columbia. *Geol. Surv. Can., Mem.* **420**.

________ & HICKSON, C.J. (1984): Crystal fractionation of the basalt comendite series of the Mount Edziza volcanic complex, British Columbia: major and trace elements. *J. Volcanol. Geotherm. Res.* **21**, 79-106.

STANLEY, C.R. & RUSSELL, J.K. (1989): Petrologic hypothesis testing with Pearce element ratio diagrams: derivation of diagram axes. *Contrib. Mineral. Petrol.* **103**, 78-89.

STASIUK, M.V. & RUSSELL, J.K. (1990): Quaternary volcanic rocks of the Iskut River region, northwestern British Columbia. *Geol. Surv. Can., Pap.* **90-1E**, 153-157.

STOUT, M.Z. & NICHOLLS, J. (1977): Mineralogy and petrology of Quaternary lavas from the Snake River Plain, Idaho. *Can. J. Earth Sci.* **14**, 2140-2156.

________ & ________ (1983): Origin of the hawaiites from the Itcha Mountain Range, British Columbia. *Can. Mineral.* **21**, 575-581.

SUN, SHEN-SU & MCDONOUGH, W.F. (1989): Chemical and isotopic systematics of oceanic basalts: implications for mantle composition and processes. *In* Magmatism in the Ocean Basins (A.D. Saunders & M.J. Norry, eds.). *Geol. Soc., Spec. Publ.* **42**, 313-345.

TSUCHIYAMA, A. (1985): Dissolution kinetics of plagioclase in the melt of the system diopside – albite – anorthite, and origin of dusty plagioclase in andesites. *Contrib. Mineral. Petrol.* **89**, 1-16.

WATSON, B.E. (1982): Basalt contamination by continental crust: some experiments and models. *Contrib. Mineral. Petrol.* **80**, 73-87.

________ & JUREWICZ, S.R. (1984): Behavior of alkalies during diffusive interaction of granitic xenoliths with basaltic magma. *J. Geol.* **92**, 121-131.

WHEELER, J.O., BROOKFIELD, A.J., GABRIELSE, H., MONGER, J.W.H., TIPPER, H.W. & WOODSWORTH, G.J. (1988): Terrane map of the Canadian Cordillera. *Geol. Surv. Can., Open File* **1894**.

________, ________, ________, ________, ________ & ________ (1991): Terrane map of the Canadian cordillera. *Geol. Surv. Can., Map* **1713A**.

WILCOX, R.E. (1954): Petrology of Paracutín volcano, Mexico. *U.S. Geol. Surv., Bull.* **965-C**, 281- 353.

WRIGHT, F.E. (1906): The Unuk River mining region of British Columbia. *Geol. Surv. Can., Summary Report of the Year 1905*, 68-74.

Received September 24, 1999, revised manuscript accepted July 1, 2000.

APPENDIX 1. TESTING FOR ASSIMILATION IN ELEMENT-RATIO DIAGRAMS

Previously, we used element-ratio diagrams (Pearce 1968) to directly test petrological hypotheses against chemical data (*e.g.,* Russell & Nicholls 1988, Russell *et al.* 1990). In most instances, the hypothesis represents a closed-system process, such as fractionation or accumulation of olivine phenocrysts (*e.g.,* Russell & Snyder 1997). In this paper, we begin with the expectation that if these basalts have behaved as closed systems, then their chemical compositions will be strictly controlled by sorting of the observed phenocryst assemblages (Ol ± Pl ± Cpx). However, we also wish to recognize the effects of assimilation of crust. The chemical signature of this process could be subtle, given the composition of rocks comprising Stikinia. Therefore, we have endeavored to make a more stringent test of the closed-system hypothesis by designing the diagram to be sensitive to specific compositions. Specifically, the numerator coefficients have been calculated using the matrix methods described by Stanley & Russell (1989) and Nicholls & Gordon (1994) so that inputs of granitic material will cause pronounced deviations from the model trend. We used the measured compositions of bulk xenoliths and associated glasses as proxies for the range of compositions of the crustal assimilant.

On the element-ratio diagram shown in Figure 7, rocks compositions that are strictly related by our closed-system process will generate a unique trend with a slope of one. The consequences of adding one of our idealized crustal contaminants to the magma composition are summarized in Figure A1. The compositions of bulk xenoliths, glasses within the xenoliths and the quartz monzonite bedrock (LF–28) have been converted to atomic proportions and normalized to eight atoms of oxygen. Figure A1 shows the X- and Y-axis displacements (A) and the slopes and norms (B) of the vectors that result from projecting these compositions into the element-ratio diagram (Fig. 7).

The norms of these projections provide a relative measure of the effect of each composition on chemical trends plotted on the element-ratio diagram. The fact that the norms are non-zero and similar in value implies that assimilation of any of these compositions will cause substantial displacements in the element-ratio diagram. The slope is the critical parameter governing whether or not the displacement will be visible. If the slope is parallel to the "closed-system" trend (*e.g.,* slope = 1.0), then the assimilation process would be virtually invisible in this diagram. As shown in Figure A1(B), most compositions will generate trends at high angles (slopes of 0 – 0.5) to the model trend. The implication is that even small amounts of assimilation will disrupt the magma chemistry in a highly visible manner. As the assimilant is being added to the system, the compositional shift will be toward higher values along the X axis (Fig. 8; see inset).

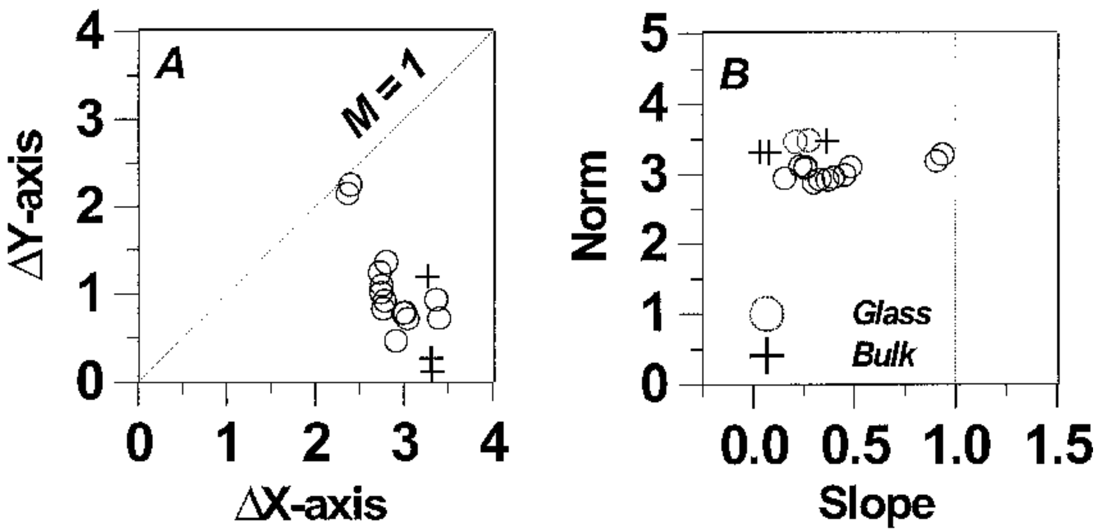

FIG. A1. The vector properties of the compositions of possible assimilants (*e.g.,* Table 3, Fig. 4) after being normalized to eight atoms of oxygen and projected onto element-ratio diagrams (Figs. 7, 8). (A) Displacement onto X and Y axes caused by assimilation of one eight-oxygen unit of each composition. The dashed line indicates equal displacements on both axes. (B) Computed slope and norm of the displacement vector caused by assimilation of one eight-oxygen unit of each composition. Most compositions generate slopes that are significantly different from 1 (*e.g.,* phenocryst-sorting process).